國立臺灣大學電機資訊學院電信工程學研究所

博士論文

Graduate Institute of Communication Engineering

College of Electrical Engineering ＆ Computer Science

National Taiwan University

Doctoral dissertation

異質性無線網路下之合作定位技術

Cooperative Multi-Radio Localization in
Heterogeneous Wireless Networks

方士豪

Shih-Hau Fang

指導教授：林宗男 博士

Advisor: Tsung-Nan Lin, Ph.D.

中華民國 98 年 1 月

January, 2009

誌謝

這本論文最先要感謝的便是我的指導教授林宗男博士，在博士班生涯中，老師對研究嚴謹的態度與邏輯的訓練讓我獲得多方面的成長，才能讓我的論文順利產生。其次要感謝李琳山教授與洪志偉教授在我碩士班時期奠立良好的基礎，讓學生在各種領域都能有所發揮。另外也要感謝口試委員張瑞雄，蔡子傑，黃仁竑，廖婉君，吳曉光與陳俊良教授們在百忙之中抽空指導並給予寶貴的意見，讓學生的論文能更臻完善。

接下來要感謝同期伙伴老王與老錢以及實驗室的同窗伯江與俊源，一路上你們的相伴是很重要的力量。感謝實驗室的震謙，浩儒，琮訓，書銘，武億，與育宏學弟們，你們所進行的量測讓我節省許多時間。接著要謝謝我的老友許肥，中午跟你一起吃飯討論小說電影與撲克技術是很有效的減壓處方。要感謝的人真的很多，牌友老曾與老蔡，球友血棒與小頭，感謝每位曾經幫助過我的貴人與生活上的同伴。

最後我要感謝我的家人。感謝老爸，老媽與我的妻子小珊。由於你們的支持我才能無後顧之憂的完成學業。僅以此論文獻給你們，希望我沒有讓你們失望。

摘要

由於手持設備的發展以及無線技術的普及，我們極有可能在未來的計算環境中利用可存取的異質性網路來提供定位服務。因此，為了能夠有效挖掘出隱藏於各種異質網路訊號中的位置資訊，我們提出了兩種合作式定位演算法。第一種演算法，我們稱之為直接式多重訊號融合 (Direct Multi-Radio Fusion)。在這個演算法中，我們利用空間轉換的觀念將各種無線技術中所帶的位置資訊進行重整。在這種情形之下，多餘並重複的資訊能夠最小化，使的重要資訊能夠去蕪存菁的被擷取出來進而提升定位系統效能。資訊重整之後，每個新成分與空間位置之間的關連性事實上並不相同。第二種演算法，稱之為合作式特徵訊號定位 (Cooperative Eigen-Radio Positioning)，便是更進一步利用此不同的相關性提升定位正確性。我們首先利用一個近似熵函數將不同的相關性進行量化，成為每一個新成分的鑑別度指標。在定位演算時，具有高指標的成分便賦予較高的信心水準。因此，各成分能夠各司其職，依據其所對應的鑑別度指標來評估其計算結果所應得到的權重。

在我們的合作式定位演算法，主成分分析技術被應用來選擇空間轉換的基底以及量化每個新成分與位置的相關性。本論文中，我們在真實的各種異質性網路包含手機網路(GSM)，數位電視(DVB)，類比廣播(FM)，以及無線區域網路(WLAN)實踐我們的演算法。實驗中所有的無線訊號都是來自於真正的場測。我們利用頻譜分析儀來記錄手機網路，數位電視與類比廣播的訊號以及使用筆記型電腦來進行無線區域網路的量測。實驗環境包含兩個大範圍的室外場測-台大校園與部分文山區(貓空)。室內場測則包括台灣大學博理館 5F 的環境。實驗結果顯示我們所提出的合作式定位演算法與傳統的訊號融合法比較，能夠降低 44.19%至 48.88%的 50%誤差圓徑(circular error probable)以及 48.25%至 67.17% 的 67%誤差圓徑。

Abstract

Recent advances in mobile devices and ubiquity of wireless infrastructures create the opportunity to utilize heterogeneous wireless networks (HWNs) for the localization. To efficiently exploit the spatial correlation embedded in the RSS (received signal strength) measurements from HWNs, we proposed two algorithms via a cooperative approach. The first algorithm, called Direct Multi-Radio Fusion, tries to discover the spatial correlation after the information of measurements is reorganized in order to minimize the redundancy among different wireless radio technologies. After the reorganization, each new component contains different amounts of correlation with respect to the location estimation. The other algorithm, called Cooperative Eigen-Radio Positioning, takes a step further to incorporate the spatial discrimination property to efficiently estimate the location information.

In our location system, principal component analysis is utilized to not only reorganize the information but also quantify the spatial discrimination from an information theoretical perspective. We have implemented our algorithms for different wireless technologies involving the cellular GSM, DVB, FM and WLAN. All data are actual measurements obtained by commercially available equipment and all experiments are conducted in realistic outdoor/indoor environments in-

cluding the campus of National Taiwan University (NTU), Wen-Shan rural area and BL building in NTU. The results show that the proposed algorithm reduces 44.19-48.88% and 48.25-67.17% of the mean error and 67% circular error probable, respectively, as compared to the conventional approaches.
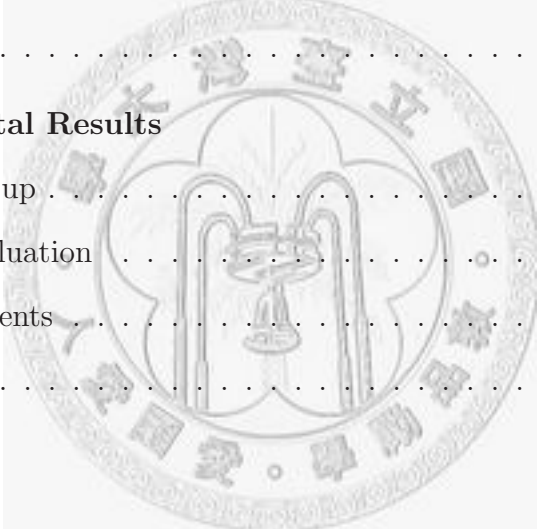
Contents

i

List of Figures

List of Tables

Chapter 1

Introduction

The demand for location-based services (LBSs) has been driving the need for the accurate positioning techniques in the past and is expected to remain the same in the future [1–3]. Although Global Positioning System (GPS) has been in service for many years, it still requires built-in GPS receiver and needs support in urban and indoor situations [4]. Thus, location estimation based on existing wireless communication infrastructure has advanced rapidly in recent years [5, 6]. For example, the localization mechanisms using cellular technologies such as Global System for Mobile communication (GSM) and Code-Division Multiple Access (CDMA) standards are attractive options in terms of their popularity [7–9]. Wireless LAN (WLAN, 802.11) also attracts much interest in indoor positioning recently [10, 11].

Today's mobile devices offer multiple wireless technologies such as the cellular networks (GSM/2.5G/3G), WLAN and Bluetooth. More technologies, such as DVB (digital video broadcasting) and WiMax (worldwide interoperability for microwave access, IEEE 802.16) are expected to be equipped with the future mobile devices. This will create the opportunity to utilize heterogeneous wireless

networks (HWNs) to localize the user [12]. The practical benefit is that users can be served with more accurate and fantastic LBSs. Once the multi-radio from HWNs is available, a cooperative positioning mechanism can combine the strength and compensate the limitations of various wireless technologies. For instance, the number of GSM base stations is likely to be limited in a rural area. At such conditions, the performance of an individual GSM-based system is limited due to the finite information. On the contrary, the performance of combining information from multiple network architecture can be easily improved to meet the user's requirement because the abundant information from HWNs can be utilized.

This article focuses on the received signal strength (RSS) from heterogeneous wireless networks instead of the different signal features in a homogeneous network [13–15]. Such RSS-based approaches are economic and compatible for the existing wireless networks because of the indispensable RSS sensing function [16]. However, the heterogeneity of RSS definitely exists due to the different standardizations and radio properties. This phenomenon makes the asymmetric contribution of each RSS and thus, increases the difficulties of a hybrid localization system design. Traditional RSS-fusion algorithms try to combine the estimated results from multiple technologies by an average [17] or a minimum mean square error (MMSE) sense weighting, namely SELFLOC (selectively fuses location information) algorithm in [18]. The performance can be improved under the assumption that the random error can cancel each other out. However, such combined methods only consider the performance of each network independently. For example, if GSM and DVB are available and GSM performs much better than DVB. Then the weighted result is certainly dominated by GSM. This way, the hidden location

information of DVB that can compensate GSM is not exploited effectively due to the much lower weights. Moreover, the information may be duplicated due to the correlation of the measurements when more technologies are involved. Such duplicated information may incur an biased location estimate [19]. In this context, an important issue is how to jointly cooperate various information sources from HWNs in an intelligent manner to achieve a higher accuracy. While many studies have done on the wireless positioning, fusing multiple information from HWNs for localization is still largely missing.

In this thesis, we propose a cooperative mechanism to efficiently exploit the location information embedded in the RSSs from heterogeneous wireless radio technologies. Measured information is first reorganized to make sure the repeated information between each other is minimized. Therefore the location information can be more easily exploited. Furthermore, each member contains different contents of location information after the reorganization. We take a further step to quantify the location discrimination with respect to each component to efficiently utilize the available information to improve the accuracy performance. We have designed and implemented our algorithms in different HWNs by using realistic GSM, DVB, FM and WLAN RSS measurements in both outdoor and indoor environments. Significant improvement has been obtained in all of our experiments, which demonstrates our contribution and the success of our algorithms.

The main contribution of this thesis is five folds: (a) We show that, by projecting the measured multi-radio into a decorrelated signal space, the positioning accuracy is improved since the duplicated information between measurements of HWNs is reduced after the reorganization. (b) Three classical decorrelated transformation techniques including Discrete Cosine Transform (DCT), Princi-

pal Component Analysis (PCA), and Independent Component Analysis (ICA) are compared in a homogeneous wireless environment. We find that PCA achieves the best performance on the location fingerprinting task. (c) We demonstrate that our approach achieves a more efficient information compaction and provides a better scheme to reduce various system cost such as the online computation, data transmission, required storage and necessary training samples. (d) We define the new variables, named discriminative gains, to represent the unequal importance of each member after the transformation. Experimental results in different HWNs show that the accuracy can be greatly enhanced when each technology is intelligently cooperated each other according to its discriminative gains. (e) We provide not only a method to quantify the importance but also a quasi entropy function to assign the appropriate discriminative gains from the estimated importance.

In the following chapter, we illustrate the physical properties of the RSS measurements and the location fingerprinting systems. We review the related works including the RSS fusion approaches and the importance quantification methods for information selection. We also indicate a gap in the previous research.

Chapter 3 studies several decorrelated transformation approaches for information reorganization. We carry out comparisons with three classical decorrelated spaces including DCT [20,21], PCA [22,23] and ICA [24,25]. Two traditional RSS selection criteria: MaxMean [26] and InfoGain [27] are also compared. Initial results are presented in a homogeneous wireless network and several accomplished advantages are discussed as well.

Chapter 4 proposes two cooperative positioning algorithms. The first is Direct Multi-Radio Fusion (DMRF) where the information is reorganized in a trans-

formed space. The transformation cancels the duplicated information by combining each RSS such that the location information can be more effectively extracted. The second is Cooperative Eigen-Radio Positioning (CERP) which further takes the different importance into consideration. The contribution of the reorganized information is considered discriminatingly and quantified for the positioning utilization.

In Chapter 5, we implemented our algorithms in different HWNs of both outdoor and indoor environments. The former consists of GSM, DVB and FM while the latter includes WLAN and GSM. All RSS data of HWNs are actual measurements obtained by commercially available spectrum analyzer and wireless cards. All experiments are conducted in realistic environments including the campus of National Taiwan University (NTU), Wen-Shan rural area and the fifth floor of BL building in NTU. The results show that the proposed algorithm outperforms each single-network based approach and traditional RSS-fusion algorithms. The significant reduction of mean error and 67% CEP are 44.19-48.88% and 48.25-67.17%, respectively, as compared to the existing algorithms.

Finally, the results obtained in those chapters are summarized and conclusion are made in Chapter 6. Some future works are also given in the chapter.

Chapter 2

Location Fingerprinting Systems

This chapter first presents an overview of various wireless positioning architectures. Then, we focus on the location fingerprinting systems, which belong to a RSS-mapping approach. Based on the pre-recorded RSS from different locations, denoted as *fingerprints* or *radio map*, the user's location is estimated by mapping the currently measurement with the pre-stored fingerprints. The physical properties of RSS and various mapping algorithms are presented in this chapter. Besides, some related works are further investigated. We study existing importance quantification methods for RSS selection and also indicate a gap of those approaches. We point out that the repeated information should be considered and the information lost should be also minimized while selecting the RSSs for positioning.

2.1 Wireless Position Estimation

With accurate location knowledge, many useful applications such as personal safety, content delivery and intelligent transport system can become feasible [28–31]. Such LBS has been predicted to be a huge market in the coming future
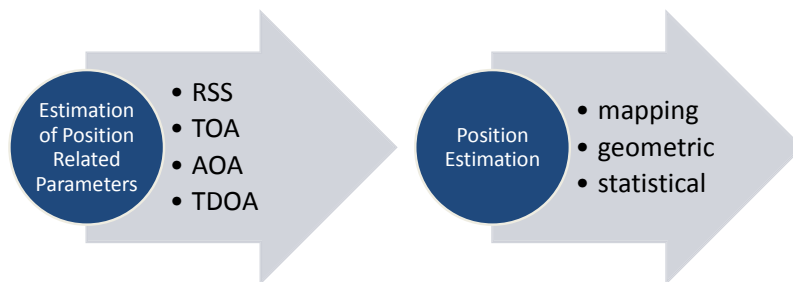
Figure 2.1: The architecture of the wireless position estimation systems

.

and recognized by IEEE. Many standardizations such as 802.11v and 802.15.4a are designed with the localization capabilities [32–34]. Besides, the Federal Communications Commission (FCC) in the US has even ruled for all devices that 67 percent of position estimations should be less than 50 meters to facilitate emergency services (Enhanced 911) [35].

Recently, positioning in wireless networks has drawn considerable concern to enhance the positioning accuracy and to increase the service coverage [36]. For example, cellular GSM [37–39], FM [40–42] and DVB technologies [43, 44] have been performed for outdoor location while Radio Frequency Identification [45], WLAN [46–48] and Bluetooth [49] have been widely studied in indoor positioning. Sensor networks [50,51] and ultra-wideband (UWB) [3,52,53] technologies are also considered of great importance.

In each wireless network, various signal parameters such as RSS, time of arrival (TOA), angle of arrival (AOA) and time difference of arrival (TDOA) are estimated and exchanging between the device and the reference transmitters [54,55]. Then, the estimated signal parameters are used to find location by different methods such as the mapping, geometric and statistic approaches [34,56,57]. The basic

architecture of the wireless positioning is shown in Fig. 2.1. In fact, each method has its own limitations and advantages depending on the accuracy requirements, system constraints and infrastructure coverage. For example, the angle and timing signal parameters are useful for positioning; however, the accurate measurements are not easily available [33]. Although mapping-based approach requires a previously stored database, this approach provides a high accuracy in challenging wireless environments [56]. This thesis focuses on the RSS-mapping approach, which is called the location fingerprinting. The fingerprinting approach usually uses the most commonly signal, the power, commonly referred to as RSS, to provide a distance and location information depending on a database (training data). In the following sections, we will briefly describe the physical properties of the RSS signals and the location fingerprinting systems.

2.2 Physical Properties of RSS

Based on the radio propagation model [58, 59], the free space loss of the signal power can be calculated by Friis equation [60]

$$L = \left(\frac{4\pi d}{\lambda} \right)^2 \tag{2.1}$$

where L is the free-space path loss, λ is the wavelength of an electromagnetic wave, and d is the distance between the sender and the receiver. Such property shows there exists a relationship between the receiving power and the distance, and that explains why RSS can be utilized for the wireless positioning. However, the relationship between RSS and distance in a real world is difficult to model. For example, the most simple log-distance path loss model [58] is
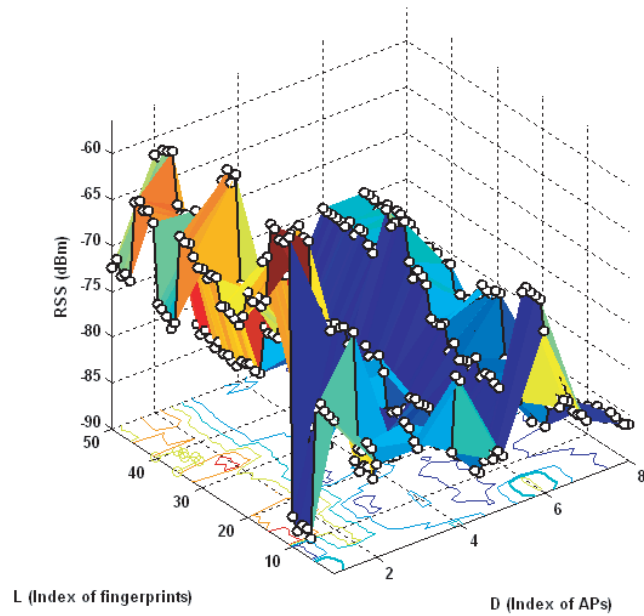
(a) The collected WLAN RSS for a certain location.
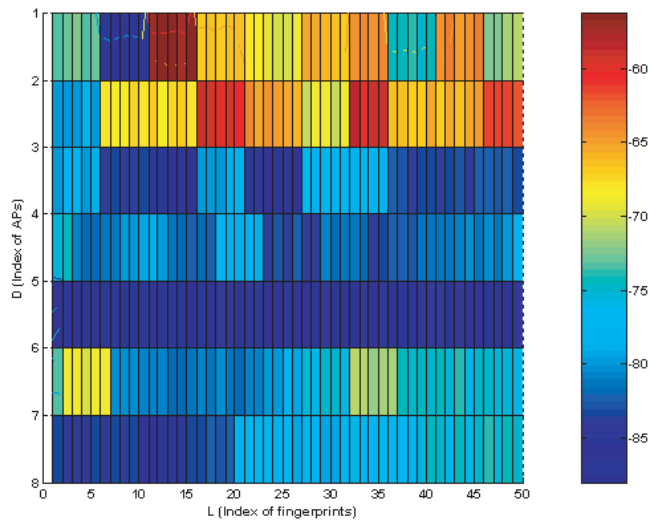
(b) A 2D projection of Fig. 2.2(a)

Figure 2.2: A visual picture of the collected WLAN RSS at a fixed indoor location based on temporal and access point diversity.

$$\overline{PL}(d)[dB] = PL(d_0)[dB] + 10nlog(d/d_0) + N[dB]. \qquad (2.2)$$

where d_0 is a reference distance, n is the path loss exponent, N is the noise, and [dB] means the unit in decibels. From Eq. 2.2, the mean path loss $\overline{PL}$ is a function of distance d to the n power, which indicates how fast power loss increases with distance. However, estimating the real value of n is difficult because it is depending on the physical surroundings. In some environments, such as buildings, stadiums and other indoor environments, the path loss exponent can reach values in the range of 4 to 6. On the other hand, a tunnel may act as a waveguide, resulting in a path loss exponent less than 2. Moreover, RSS is commonly modeled to include both path-loss and shadowing effect, which is represented by the term N. This noisy effect, usually modeled as a Gaussian random variable, results in the temporal variation of RSS even at a fixed location. Several approaches such as the temporal filter or singular-value decomposition are utilized to remove the noisy effect [61]. In a NLOS (nonline-of-sight) situation, the multipath effect should be considered with an appropriate choice of channel parameters.

Theoretically, the observed RSS is composed of both a LOS component and numerous delayed signals with different attenuations. That is, RSS includes a significant contribution from numerous multipath components. All such signals combine to an alias version, which may be enlarged or diminished depending on the relative phases of the delayed reflections. Moreover, the observable reflection is affected not only by the propagation environment but also by the signal bandwidth for a band-limited system. It is possible to observe more multipath components when a larger bandwidth gives better time resolution [62]. In general, the measured RSS in a multipath induced environment can be written as:

$$x(t) = \sum_{\tau=0}^{N-1} \alpha(\tau) \cdot h(\tau) \cdot [s(t-\tau)]e^{j\phi(\tau)} + g(t) \tag{2.3}$$

where $x(t)$ means the RSS observation at time t and $h(\tau)$ and $\phi(\tau)$, respectively, represent the amplitude and relative phase of the delayed multipath components. The total number of delayed paths is equal to N-1. $\alpha(\tau)$ is a binary function that controls the on-off activity of the corresponding multipath filter $h(\tau)$, $s(t)$ is the transmitted signal and τ is the time delay. $g(t)$ is the communication noise, and in general, this noise contains everything not included in the summation term representing the multipath model. There are a number of factors causing the multipath effect such as the material and number of walls, human mobility, temperature and humidity. Those factors are jointly reflected on the model parameters $h(\tau)$, $\phi(\tau)$ and $\alpha(\tau)$.

Several works have investigated the estimating problem in a NLOS environment [63–66]. However, predicting an accurate RSS in a realistic world is still a complex problem, especially for an indoor environment. A visual picture of such radio data for a certain indoor location is plotted in Fig. 2.2. Fig. 2.2(a) shows the radio fingerprints for a fixed location based on temporal and access point (AP) diversity. As can be seen, the temporal variation of each AP is varying due to the different multipath propagation environments. Fig. 2.2(b) shows a 2D projection with different colors, where the temporal variations of RSS can be more clearly observed from its rows. The difficulty of predicting accurate RSS from the distance motivates the technology of *location fingerprinting*, having the advantage of providing a high accuracy in both LOS and NLOS scenarios. This technology is then presented in the following section.

2.3 Location Fingerprinting

	Bahl et al. (2000): RADAR	Youssef et al. (2003,…,2005): Horus	LaMarca et al. (2005): Place Lab	Lorincz et al. (2005): MoteTrack
organization	Microsoft Research	University of Maryland's	Intel Research	Harvard University
Scale	Building	Building	City	Building
Measurements	WLAN	WLAN	WLAN &GSM	IEEE 802.15.4

Figure 2.3: Examples of current radio location fingerprinting systems
.

Location fingerprinting is a promising wireless positioning technology, having the major advantage of providing a high accuracy in challenging wireless environments. Based on a database of pre-recorded measurements of network characteristics from different locations, denoted as *fingerprints* or *radio map*, the user's location is estimated by mapping the currently measurement with the pre-stored fingerprints. Fig. 2.3 shows some examples of current radio location fingerprinting systems. Most existing systems are aimed at the indoor buildings since the database management is more easy. Currently, this approach is extended to a city-wide area as proposed by the Place Lab. In general, two stages of the fingerprinting are the offline modeling and the online positioning [56] and they are presented as follows.

2.3.1 Offline Stage

During the offline stage, a site survey performed in the target environment is required to collect the network characteristics. The characteristics are typically RSS and are collected at sampling locations to build the radio map. A radio map
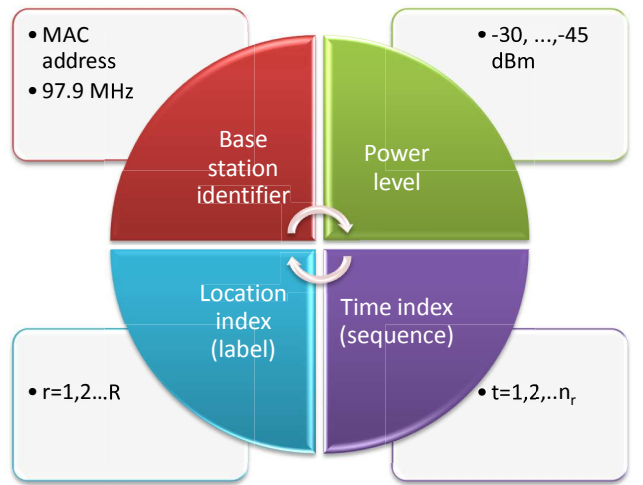
Figure 2.4: The four dimensions in the radio map
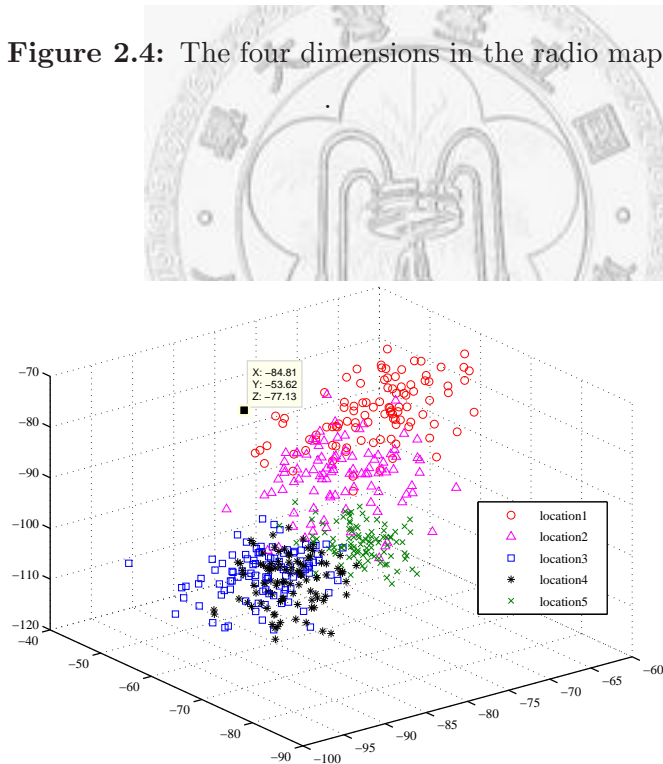
Figure 2.5: A visual picture of the collected fingerprints including 3 information sources, 5 locations and 50 samples RSS at each location

thus provides a model of RSS in a development area. In general, the radio map contains at least four dimensions, as shown in Fig. 2.4. First, the base station identifier means the source of the RSS signal. For example, the MAC address is used for WLAN positioning while the used frequency is recorded for FM or GSM location systems [67]. Second, the power level, usually reported in decibels, indicates the numerical value of RSS. Note that the distribution of RSS tends to a log-normal distribution, as indicated by Eq. 2.2. Third, the time index t represents the order of the measurements of RSS. We usually collect a sequence of RSSs, each sequence contains n_r samples per location to observe its temporal variation. Finally, the location index means where you collect RSS. The more reference locations R means the higher density in the radio map at the expense of more collecting effort. A visual picture of the collected fingerprints is reported in Fig. 2.5. This figure shows a typical radio map includes 3 information sources, 5 locations and 50 samples RSS at each location. After constructing the radio map, a wireless client's is estimated by inspecting currently measured RSS. We describe several location estimation methods in the next subsection.

2.3.2 Online Stage

During the online stage, the positioning techniques measure RSS in real-time and estimate the location based on the measured RSS and the previously stored radio map. The fundamental objective is seeking a mapping between the radio measurements to a physical location. One of the most popular mapping function is the probabilistic models [68, 69]. The main idea can be regarded as finding $p(\mathbf{l_r}|\mathbf{X})$, where $\mathbf{X}$ is an observed RSS vector, $\mathbf{l_r}$ represents the r-th reference location in the radio map and $p(\mathbf{l_r}|\mathbf{X})$ indicates the posteriori probability of location

2. LOCATION FINGERPRINTING SYSTEMS

l_r given the observation $\mathbf{X}$. By means of Bayes' rule, $p(\mathbf{l_r}|\mathbf{X})$ depends only on the likelihood $p(\mathbf{X}|\mathbf{l_r})$ when the prior probability $\mathbf{p(l_r)}$ follows a uniform distribution. Thus, the location can be regarded as a multivariate multiple regression problem [19] and estimated as

$$\widehat{\mathbf{l}} = \sum_{r=1}^{R} \mathbf{l_r} \cdot p(\mathbf{X}|\mathbf{l_r}) \tag{2.4}$$

where R is the number of reference locations and $\widehat{\mathbf{l}}$ represents the estimated result. Several methods can compute the likelihood function $p(\mathbf{X}|\mathbf{l_r})$ from data such as the Gaussian approximations [70], histogram methods [69] and kernel functions [19, 71]. The Gaussian approximation methods estimate the mean u_d and variance σ_d first and then compute $p(\mathbf{X}|\mathbf{l_r})$ as $\prod_{d=1}^{D} \frac{1}{\sqrt{2\pi}\sigma_d} \exp\left(\frac{-(x_d - u_d)^2}{2\sigma_d^2}\right)$ under the Gaussian assumptions. The histogram method requires that we fix a set of bins, i.e., a set of non-overlapping intervals that cover the whole range of the variable $\mathbf{X}$. Then the probability is the value of the density function within each of the bins. In the kernel method, the probability is assigned to a kernel function around each of the observations in the training data.

$$
\begin{aligned}
p(\mathbf{X}|l_r) &= \frac{1}{n_r} \sum_{t=1}^{n_r} \hat{K}(\mathbf{X}, \mathbf{X}_r(t)) \\
&= \frac{1}{n_r} \sum_{t=1}^{n_r} \frac{k(\mathbf{X}, \mathbf{X}_r(t))}{\sqrt{k(\mathbf{X}, \mathbf{X})k(\mathbf{X}_r(t), \mathbf{X}_r(t))}}
\end{aligned}
\tag{2.5}
$$

where n_r is the number of collected RSS at the r-th location and $\mathbf{X}_r(t)$ is the t-th collected RSS at the r-th location. The function $k()$ and $\hat{K}()$, respectively, indicate a certain nonlinear kernel and its normalized form. The widely used Gaussian Radial Basis Function (RBF) is defined as

$$k(\mathbf{X}, \mathbf{X}_r(t)) = \exp\left(\frac{-1}{2\sigma_r^2}||\mathbf{X} - \mathbf{X}_r(t)||^2\right) \tag{2.6}$$

where σ_r is an adjustable width and the operation $||(\cdot)||$ represents the norm function. The most commonly used L^2 norm is adopted which represents the Euclidean distance as $(||\mathbf{X}|| = \sqrt{x_1^2 + \cdots + x_D^2})$.

In addition to the probabilistic method, several pattern matching algorithms have also been applied to learn the relationship between RSS and the client's position such as the nearest-neighbor [46], neural networks [16, 72, 73], and support vector machine [74]. The nearest-neighbor method finds location by comparing the distance between two vectors as $\widehat{\mathbf{l}} = l_r$, $\mathrm{r} = \underset{r}{\arg\min}\, D(\mathbf{X}, \mathbf{X}_r(t))$, where D is some specified distance measure function. Neural network is composed of a number of interconnected units (neurons) in parallel to nonlinearly map the output from the input (RSS). The location is estimated based on the emitted output of each unit, which is calculated by the chose activation function and adjustable weightings. An adaptive neural network is proposed in [75], which incrementally inserts the discriminative components and recursively updating the weightings in the network until no further improvement is required. Support vector machine maximums the margin between locations when modeling the radio map. This technique also shows tolerance for the incompleteness of the RSS signals.

To improve accuracy, some additional signals are measured and combined with RSS. For instance, Nerguizian et al. [16, 76] further use a measured channel impulse response and King et al. [77] additionally utilize the orientation of the user by a digital compass. Recently, Intel [33] proposes a TOA-enhanced approach by firmware and silicon modifications and Yin et al. [45] work out a location system where the radio map is temporally update.

Furthermore, many challenging issues in location fingerprinting are important such as the scalability and the system cost [11, 56, 78]. For example, PlaceLab [79] employs the cellular-based radio and investigates the fingerprinting in a metropolitan scale environment. To reduce the labor cost of collecting fingerprints, Chai et al. [80, 81] propose a learning-based approach utilizing unlabeled samples and Moraes et al. [82] study a calibration-free location system. To minimize the communication cost between a client and a server, a neural network approach is proposed [73] and a zone-based reporting is utilized in [83]. A fingerprints-selection approach is proposed [84] to avoid the time-consuming task of copying all fingerprints.

In the next subsection, we focus the previous research of importance quantification methods, which aim at selecting suitable RSSs for localization.

2.3.3 Importance Quantification for Information Selection

The importance quantification methods are originally designed for information (RSSs) selection. In these methods, some importance evaluation function is used to rank the sensed RSSs according to their estimated importance. Then, the more important RSSs/information are selected for positioning. This way, several advantages can be accomplished such as improving the speed of positioning, better power efficiency, reducing the storage requirement and avoiding the problem of overfitting. For example, Youssef et al. [26] utilized the strongest RSSs to decrease the computational complexity of the positioning algorithm. Chen et al. [27] worked out a method for selecting the most discriminative RSSs with the advantage of power efficiency. When the positioning algorithm is performed on the handheld devices, extra care should be taken due to their constrained resource.

Clearly, choosing a subset of RSSs is an intuitive way to reduce the computational burden and storage requirement on the resource-weak devices. Conserving power is also an important benefit since recharging batteries is difficult in many cases.

More importantly, the results in [27, 45] showed that the best positioning accuracy can be produced by using a subset of RSSs in a fingerprinting system. This occurs because, as the number of RSSs increases, more information is added whereas more noise is incurred [45]. Kushki et al. [19] pointed out that the distinct transmitters may produce similar measurements, leading to biased estimates and redundant computation. These works motivate the use of information selection techniques from the view point of performance.

Now, we describe those importance quantification methods in more detail. The works in [26, 85] directly utilized the value of RSSs for the estimated importance. It is because, the stronger RSS may produce more reliable information due to the less noise they encounter. In other words, the signals sent from the far transmitter experience more influence of the environmental noises, and more uncertainties are added in the signal strength. Those approaches, named MaxMean, assign the higher importance to the stronger RSSs. On the other hand, the InfoGain criterion reported in [27] assigns the more importance to the more discriminative RSSs instead. A extreme case is considered in InfoGain, if some RSS is uniformly large but differ a little over all the locations, the MaxMean will rank this RSS near the front by priority although it does not contribute to distinguishing the locations. Thus, InfoGain ranks APs in descending order of their InfoGain values which are calculated as follows:

$$InfoGain(AP_d) = H(G) - H(G|AP_d) \qquad (2.7)$$

where $H(G)$ and $H(G|AP_d)$, referred to [27], implies the "entropy of the reference locations when AP_d's value is unknown", and the "conditional entropy of the reference locations given AP_d's value". Then, some variations of these approaches are studied in the recent works. For example, [86] considers both the distinctiveness and variability of RSSs to rank the RSSs. The recent work of Kushki et al. [19] offers a real-time RSS selection technique which minimizes the correlation between selected RSSs based on different divergence measurements such as Bhattacharyya distance and information potential. This approach carries out the selection on the strongest 5 APs to reduce the complexity and ensure the coverage.
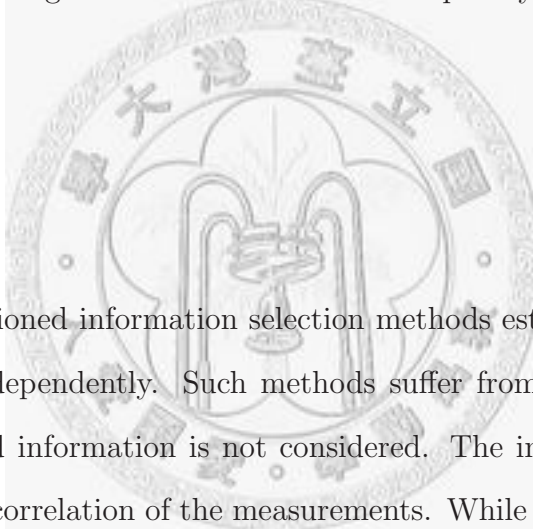
However, all the mentioned information selection methods estimated the importance of each RSS independently. Such methods suffer from two disadvantages. First, the repeated information is not considered. The information may be duplicated due to the correlation of the measurements. While quantifying the importance, we should avoid selecting RSSs which contribute the same location information. Second, those approaches discard all the information from unselected RSSs. We should minimize the lost information (maximize the retained information) while selecting important RSSs for localization. This motivates us to explore the possibility to perform the location fingerprinting in a transformed signal space in order to achieve the information reorganization and selection. The system we propose locates the clients in a transformed space and the details will be discussed in the next chapter.

2.4　Summary
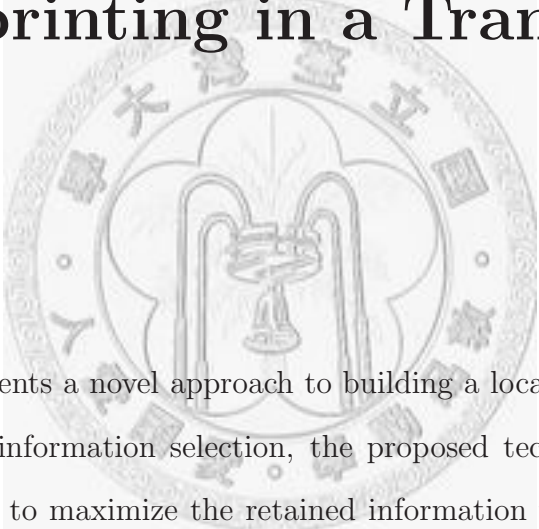
In this chapter, a taxonomy on wireless position estimation is presented. Then, we focus on the location fingerprinting, which is a promising wireless positioning technology, having the major advantage of providing a high accuracy in challenging wireless environments. The basic design of fingerprinting can be divided into two stages: the offline and online stages. During the offline stage, RSS is collected at sampling locations to build the radio map for the target environment. During the online stage, the location of the client can be estimated by comparing the measured RSS with the stored RSS values in the radio map. In this chapter, various mapping algorithms such as the probabilistic approaches are presented. Moreover, some related works are further investigated such as the importance quantification methods for RSS selection. We point out that the repeated information should be considered and the information lost should be also minimized while selecting the RSSs for positioning. This motivates us to explore the possibility to perform the location fingerprinting in a transformed signal space in order to achieve the information reorganization, as discussed in the next chapter.

Chapter 3

Fingerprinting in a Transformed Space

This chapter presents a novel approach to building a location fingerprinting system. Instead of information selection, the proposed technique reorganizes the information so as to maximize the retained information while removing parameters as more as possible under the same accuracy constraint. Our algorithm intelligently transforms RSS into a decorrelated space such that the information of all RSSs is more efficiently utilized. We carry out comparisons between three classical decorrelated techniques including DCT, PCA, ICA and two existing RSS selection methods. Testing on a homogeneous wireless environment, we find that PCA achieves the best performance on the location fingerprinting task. Moreover, several benefits of our algorithm are demonstrated such as reducing computation (better power efficiency) and requiring fewer training samples.

3.1 Purpose

Previous chapter has illustrated several importance quantification methods for RSSs selection so as to reduce the online computation, improve the speed of positioning, decrease the power consumption and the storage requirement. However, such advantages usually come at the expensive of performance. In other words, the traditional information selection techniques suffer from a critical disadvantage: it discards all the information from unselected RSSs. Only the information from selected RSSs is retained for the positioning whereas the information in unselected RSSs is totally discarded.

The question is: is it possible to reduce the online computation while keeping the whole RSS's information? This motivates us to explore the possibility to perform the location fingerprinting in a transformed signal space in order to achieve the information reorganization and dimension reduction. The goal of our work is to minimize the lost information (maximize the retained information) while removing parameters as more as possible under the same accuracy constraint. From information-theoretical viewpoint, if the RSSs are statistically correlated, the redundancy abounds among the related RSSs. If such redundancy is well exploited, it could allow a substantial data reduction while minimizes the information lost.

In general, the idea of RSS selection can be expressed in a simple mathematical form as follows:

$$
\begin{pmatrix} y_1 \\ \vdots \\ y_{D'} \end{pmatrix}_{D'*1} = \begin{pmatrix} 1 & 0 & \cdots & \cdots & 0 \\ 0 & 1 & \cdots & \cdots & 0 \\ \vdots & \vdots & \vdots & \vdots & \vdots \\ 0 & \cdots & 1 & \cdots & 0 \end{pmatrix}_{D'*D} \begin{pmatrix} x_1 \\ \vdots \\ x_D \end{pmatrix}_{D*1} \tag{3.1}
$$

where the vector, $\mathbf{X} = [x_1, x_2, ...x_D]^T \in \Re^{D*1}$, represents the measurement from available D RSSs, the matrix, $\mathbf{A} \in \Re^{D'*D}, D' \leq D$, contains the selective weight-

ing describing which RSSs are chosen, and the vector, $\mathbf{Y} = [y_1, ...y_{D'}]^T \in \Re^{D'*1}$, represents the measurement from the selected RSSs. In Eq.3.1, the first D' RSSs among $\{x_1, ...x_D\}$ are chosen and thus $\{y_1, ...y_{D'}\} = \{x_1, ...x_{D'}\}$. Unlike the zero one weighting (binary decision) in the selection of RSSs, our concept considered here is combining RSSs in order to reduce required computation while ensuring the performance of accuracy. As shown in Eq.3.2, the components $[y_1, ...y_{D'}]^T$ are produced by a transformation with real numbers. With appropriate weightings, the information transmitted into $\mathbf{Y}$ from $\mathbf{X}$ can be maximized.

$$
\begin{pmatrix} y_1 \\ \vdots \\ y_{D'} \end{pmatrix}_{D'*1} = \begin{pmatrix} a_{11} & a_{12} & \cdots & a_{1D} \\ a_{21} & a_{22} & \cdots & a_{2D} \\ \vdots & \vdots & \vdots \\ a_{D'1} & a_{D'2} & \cdots & a_{D'D} \end{pmatrix}_{D'*D} \begin{pmatrix} x_1 \\ \vdots \\ x_D \end{pmatrix}_{D*1}
\tag{3.2}
$$

The proposed method is based on the decorrelated transformation technique. The technique can identify the redundancy behind multiple variables in order to obtain a compact description of it. This is achieved by transforming RSSs to a new set of variables, which are uncorrelated and ordered by its information quantity in the transformed space. It has been proven in several applications that the same algorithm may obtain better results in a decorrelated space. For instance, JPEG compression [20] and color demosaicking [87] are operated in DCT and spectral color difference space respectively. In face recognition, PCA has been a widely used technique [22]. Our preliminary study has showed its efficiency in indoor localization [88]. In speech analysis, ICA is utilized for separating mixed audio signals into independent sources [24].

The first work utilizes the transformation technique for localization is presented in [89, 90]. Kernel canonical correlation analysis (KCCA) is used to maximize the correlation between the physical location and signal space, thus a more

accurate mapping function can be constructed. In contrast to that approach, our work aims at minimizing the correlation between each component in the signal space.

In this chapter, we show that, by projecting the measured signals into a decorrelated signal space, the positioning accuracy is improved since the cross correlation between each RSS is reduced. Besides, this novel approach achieves a more efficient information compaction and provides a better scheme to reduce the online computational complexity. The whole location information can be utilized in our approach since each component in the decorrelated space is the linear combination of all RSSs with different weights. In other words, we use the concept of feature extraction instead of feature selection to reduce the dimension required in the positioning algorithm.

In the following section, we illustrate three classical decorrelated techniques including *Discrete Cosine Transform* (DCT) [20, 21], *Principal Component Analysis* (PCA) [22, 23] and *Independent component Analysis* (ICA) [24, 25].

3.2 Decorrelated Transformations

Traditional approach builds the model and estimates location in RSS space whereas our approach is constructed in a decorrelated signal space. Define a transformation matrix, $\mathbf{A} = \{a_{d'd}\} \in \Re^{D'*D}, D' = 1, 2, ...D$, where D' represents the retained basis number. The basis for new signal space is each row vector of the transformation matrix $\mathbf{A}$ and the transformed output value can be obtained by projection to each basis.

Now the problem is how to determine $a_{d'd}$. Several techniques have been

proposed to find a set of transformation coefficients in order to achieve information reorganization and dimension reduction. For instance, the coefficients of A can be used as a typical Discrete Cosine Transform (DCT), which is a popular approach for color image compression as

$$a_{d'd} = cos(\frac{\pi}{D}(d - \frac{1}{2})(d' - 1)) \tag{3.3}$$

In DCT, each basis is a cosine wave uncorrelated to each other. Other approaches design the transformation based on the measured data such as Principal Component Analysis (PCA) and Independent Component Analysis (ICA). In PCA, $a_{d'd}$ can be determined by finding the eigenvectors $\mathbf{e}_d$ of $\mathbf{S}_\Sigma$.

$$\mathbf{S}_\Sigma \mathbf{e}_d = \lambda_d \mathbf{e}_d \tag{3.4}$$

where $\mathbf{e}_d$ is the d-th eigenvector, λ_d is the corresponding eigenvalue to $\mathbf{e}_d$ and the matrix $\mathbf{S}_\Sigma$ is the covariance matrix of $\mathbf{X}$ computed as

$$\mathbf{S}_\Sigma = \frac{1}{R \cdot n_r} \sum_{r=1}^{R} \sum_{t=1}^{n_r} (\mathbf{X}_r(t) - \bar{\mathbf{X}})(\mathbf{X}_r(t) - \bar{\mathbf{X}})' \tag{3.5}$$

This way, $a_{d'd}$ is in fact the components of $\mathbf{e}_{d'}$. The method has been shown to be the optimal linear transformation for keeping the subspace that has the largest variance [22]. Compared to DCT transformation, PCA not only reduces the cross correlation between each AP, but also reorganizes the information quantity accordingly. The eigenvectors in Eq.3.4 rank in descending order of corresponding eigenvalues as $\lambda_1 \geq \lambda_2 \geq ...\lambda_D$, where λ_d indicate the importance of the d-th basis in a theoretical view of point.

While the goal in PCA is to maximize the variance in the projection space, the goal of ICA is to find the representation of non-gaussian data as independent

as possible. Unlike PCA, there is no closed form to find a_{ld}, but many iterative algorithms based on different search criteria are instead. In this work, we adopt the FastICA criterion, which is a popular ICA algorithm and the matlab package is publicly available on the web site. The FastICA rule finds a direction that the projection maximizes nongaussianity. Nongaussianity is here measured by the negentropy function as

$$J(\mathbf{X}) = H(\mathbf{X}_{gauss}) - H(\mathbf{X}) \tag{3.6}$$

where $\mathbf{X}_{gauss}$ is a Gaussian random variable of the same covariance matrix as $\mathbf{X}$. In fact, the estimation of negentropy is difficult. Thus, some approximation methods have to be used such as the kurtosis-based or the moment-based approximation. For details on FastICA and the approximations of negentropy, please refer to [24, 91].

3.3 Performance Evaluation in a Homogeneous Wireless Network

This section conducts a series of experiments on the effects of the decorrelated transformation techniques in a homogeneous wireless network. We compare 2 information selection methods and 3 information reorganization approaches which are described in the previous sections. Then, the performance is evaluated in an indoor location fingerprinting system in terms of the accuracy, complexity and the size of training samples.
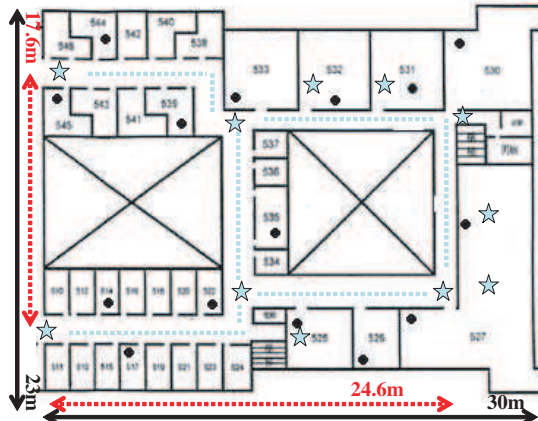
Figure 3.1: Part of the fifth floor plane of electronic engineering department of National Taiwan University, where we had performed the experiment. The dot line represents the path of data collection, the stars indicate the test rooms and the end of the test corridors, and the dots show the locations of the APs.

3.3.1 Experimental Setup

In order to evaluate the performance of the proposed technique, we collect realistic RSS data in a WLAN environment, which is characterized by a number of access points (APs) with CSMA/CA protocol. The WLAN-enabled device senses RF signals over the specified frequency band in the physical layer, and then decodes the address of APs in MAC layer such that all detectable APs are indexed [92,93]. The receiver will first attempt to decode the PHY header when the received power is greater than the physical carrier sense threshold. If the PHY header can not be decoded, the receiver will regard the medium as busy until the power level falls below the threshold. If the PHY header and MAC payload can be decoded, the receiver will operate in accordance to the 802.11 specification.

We perform the experiments in the electronic engineering department area of National Taiwan University. The dimension of the corridor is 24.6 x 17.6 meters,

3. FINGERPRINTING IN A TRANSFORMED SPACE

as shown in Fig. 3.1. Every location in this environment is covered by four to nine IEEE 802.11b APs and there are total 15 stable APs in the environment (D=15). The system performance is probably improved with a better planning. However, controlling the placement of APs is difficult because we do not have the right to move either private or public APs. This scenario just reflects the randomness of AP locations in a real 802.11 WLAN environment. We adopt an IBM ThinkPad T40 laptop as the mobile node, with RedHat 7.1 Linux operating system. A Lucent WaveLan/IEEE Wireless Card with Youssef's driver is installed to gather RSS from nearby APs. We collect 100 samples of signal strength at 86 (R=86) locations separated by 1 meter, where 81 locations are measured along 4 different corridors and 5 locations are inside the rooms. Then, we divide the collected data into 2 independent groups, where we select 41 grids (4100 samples, including 500 samples in the rooms) for 2D testing and the other 45 grids (4500 samples) for training. In that case, the grid distance is about 2 m and the test sample is never seen in the radio map.

For the validity of experimental results, we run the experiments based on an two positioning algorithm, Maximum Likelihood (ML) and Weighted K-Nearest-Neighbor (WKNN), to evaluate the performance of the decorrelated projection techniques. In ML, the probability is modified as:

$$p(\mathbf{X}|\mathbf{l}_r) = \prod_{d'=1}^{D'} \frac{1}{\sqrt{2\pi\widetilde{\Sigma}_r(d',d')}} \cdot exp\left\{\frac{-(\widetilde{x}_{d'} - \widetilde{u}_{rd'})^2}{2\widetilde{\Sigma}_r(d',d')}\right\} \tag{3.7}$$

where $\widetilde{\mathbf{X}}$, $\widetilde{\mathbf{u_r}}$ and $\widetilde{\mathbf{\Sigma_r}}$ respectively represent the transformed observation, mean vector and covariance matrix for the r-th reference location. The d'-th component of that can be formulated as follows:

$$\widetilde{x}_{d'} = \sum_{d=1}^{D} a_{d'd} \cdot o_d \tag{3.8}$$

$$\widetilde{u}_{rd'} = \sum_{d=1}^{D} a_{d'd} \cdot u_{rd} \tag{3.9}$$

$$\widetilde{\Sigma}_r(d', d') = \sum_{i=1}^{D} \sum_{j=1}^{D} \Sigma_r(i, j) \cdot a_{d'i} \cdot a_{d'j} \tag{3.10}$$

Once the transformation matrix is available, the modified ML algorithm can be applied. The parameters of Eq.3.7 could be calculated based on the projected values by means of Eq.3.9 and Eq.3.10 during the offline stage. In WKNN, the target environment is modeled as the centroids instead of the probability distributions in ML. WKNN calculates Euclidean distances between the transformed RSS and all the centroids in the model. Then the location is estimated by linearly combining the k nearest centroids with the weight of corresponding inverse distances. The constant k is set 6 in our experiments.

3.3.2 Positioning Performance

The first experiment evaluates its performance versus different model dimensions D'. Instead of the RSS number in the traditional approach, the basis number in the projected signal space determines the model dimension in our approach. Three decorrelated spaces are compared here: DCT, PCA and ICA. Additionally, 2 RSS selection criteria: MaxMean [26] and InfoGain [27] are also compared in the decorrelated space.

Fig. 3.2(a) and Fig. 3.2(b) report the mean and variance of error with respect to different signal spaces and dimension D' respectively. Both results show that

(a)
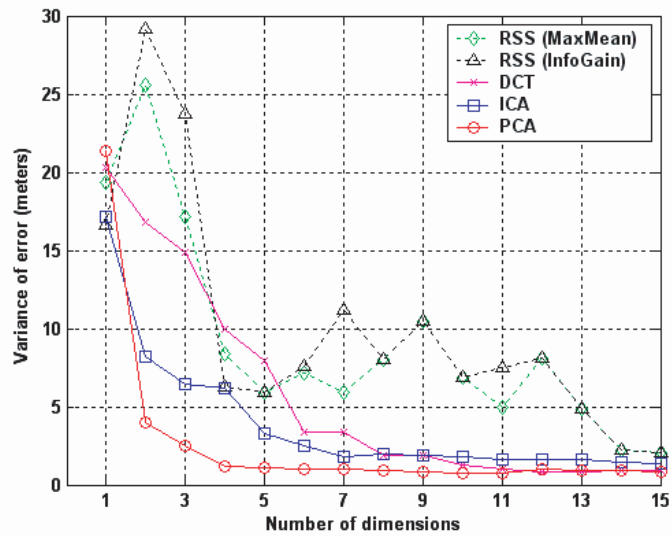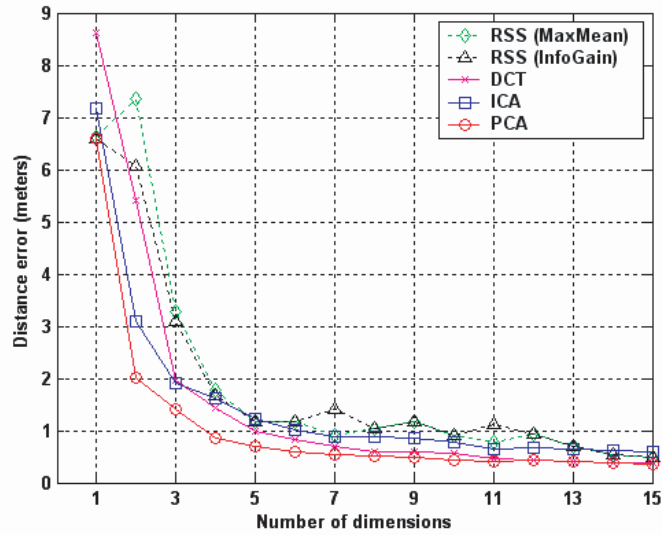
(b)

Figure 3.2: (a) Mean and (b) Variance of the estimated error versus number of APs (dimension in the decorrelated space).
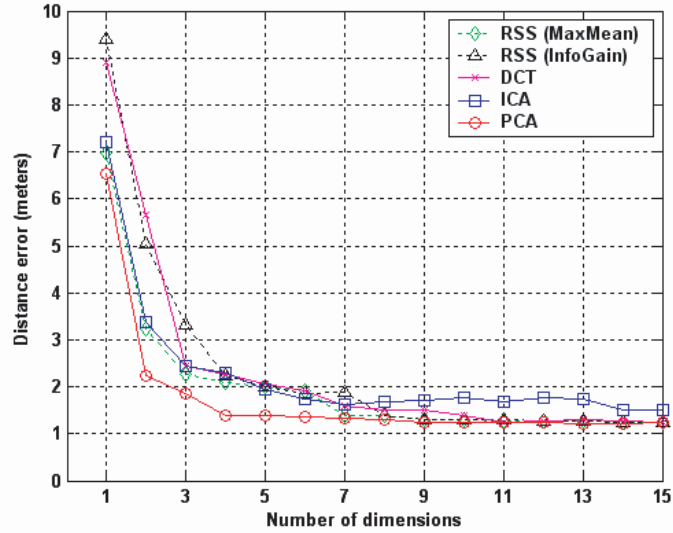
(a)
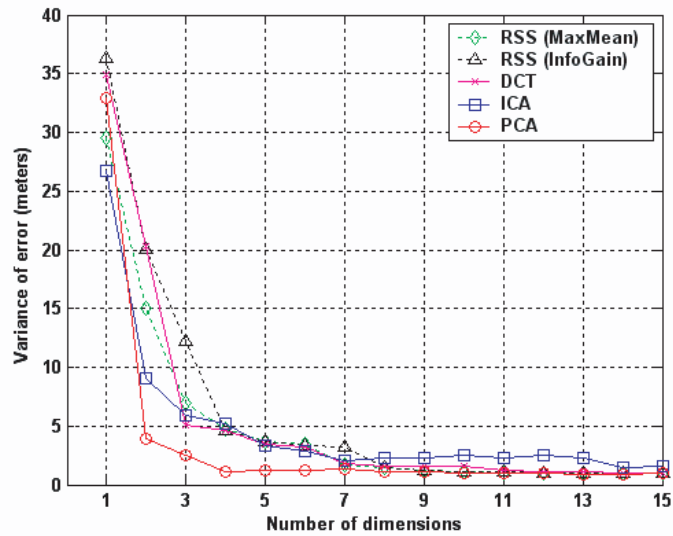
(b)

Figure 3.3: (a) Mean and (b) Variance of the estimated error versus number of APs (dimension in the decorrelated space) in the $WKNN$ based system).

mapping to decorrelated space performs much better than original RSS space, in which the two AP selection approaches are similar. The figures report that the improvement in PCA space is the most significant, especially in the lower dimension. Under 3 APs, the error mean of PCA approach is 1.41 meters while those of MaxMean, InfoGain, DCT, ICA are 3.27, 3.10, 1.97 and 1.91 meters respectively. Compared to DCT and ICA, PCA has a natural property that the basis is ranked based on the corresponding eigenvalue obtained in Eq.3.4. These eigenvalues quantize the information contribution of each basis in the decorrelated space. The bigger the eigenvalue is, the more information the basis has. Therefore PCA based decorrelation algorithm utilizes the maximal information in the positioning system at the same dimension constraint. That's the reason why PCA achieves the best performance among the compared decorrelation techniques. Furthermore, if the whole AP's information is utilized, the performance is still better and presented in the variance of error, which is 0.86 meters in PCA space while those of RSS space is 2.09 meters.

WKNN-based model is also run with the same decorrelated projection techniques in Fig. 3.3(a) and Fig. 3.3(b) for the validity of experimental results, where the mean and variance of error are reported individually. Fig. 3.3(a) and Fig. 3.3(b) clearly present a consistent result as compared to Fig. 3.2(a) and Fig. 3.2(b). That is, positioning in a decorrelated space provides better accuracy under the smaller number of dimensions, and PCA achieves the best performance among the compared techniques. That means the PCA-based decorrelated projection is useful to different back-end positioning algorithms. Besides, the optimum result obtained by WKNN is a little worse than that from ML, as shown in Fig. 3.2(a) and Fig. 3.3(a). It can be attributed to that the ML-based modeling

takes the temporal RSS variation into account while WKNN based modeling only considers the centroids of RSS. When the dimension is reduced to the minimum requirement for positioning ($D'=3$), 23.89% (1.8525 to 1.41 meters) reduction of error mean is obtained by ML technique. In other words, we still recommend the ML-based modeling for smaller dimensions, although the performance difference is minor when full APs are utilized. If the dimension can be reduced while achieving a high accuracy, an important advantage of saving computation is accomplished substantially. This issue is described in the next subsection.

3.3.3 Computational Complexity
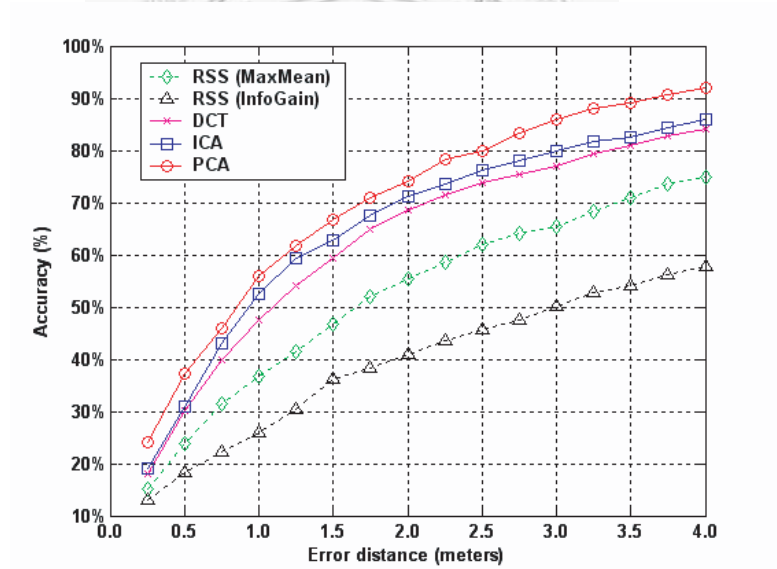
Figure 3.4: Accuracy versus error distance under 3 AP numbers condition

In ML based positioning system, the most time consuming and complicated part is the calculation of the exponential function $e(\cdot)$ in Eq.3.7. It requires 20 operations (10 addition and 10 multiplication) if a 10 order Taylor series is approximated. In that case, the likelihood calculation requires 25 operations (11

addition and 14 multiplication) for each component and thus once positioning request requires 25*15*86=32250 operations (14190 addition and 18060 multiplication) in our system, where 15 represents the number of APs and 86 represents the number of reference locations. It is intuitive to use as many APs as possible to improve the system accuracy. However, the increased AP numbers increase the online computational complexity and power demand in the client side.

To find the trade-off between the number of used APs and the accuracy can be achieved, AP selection technique is proposed to reduce the online computation. However, the disadvantage is that it may lost important information and thus leads a worse performance as shown in Fig. 3.2(a). The mean of error is 0.5m and 3.10m while 15 APs and the most discriminative 3 APs are used respectively. That is, the 80% compuational saving is at the cost of system accuracy.

Our proposed technique overcomes this drawback since we reduce the dimensionality by combining features. Fig. 3.2(a) reports that if we want to be below a 1.5m distance error, the AP selection technique requires at least 5 APs whereas PCA space needs only 3 bases. Therefore our approach has the advantage that using the fewest operations to achieve the same accuracy. It should be emphasized that the additional computation incurred by our approach is minor since the linear combination is simple to compute. The extra computation is the decorrelated transformation for the online measured RSS in Eq.3.8, which requires 30 operations (15 addition and 15 multiplication) for each decorrelated projection.

Fig. 3.4 reports the accuracy between different spaces while 80% operations are saved (D'=3). To be more specific, AP selection technique requires 25*3*86=6450 operations (2838 addition and 3612 multiplication) while our approach requires 6450+30*3=6540 operations (2883 addition and 3657 multiplication) under this
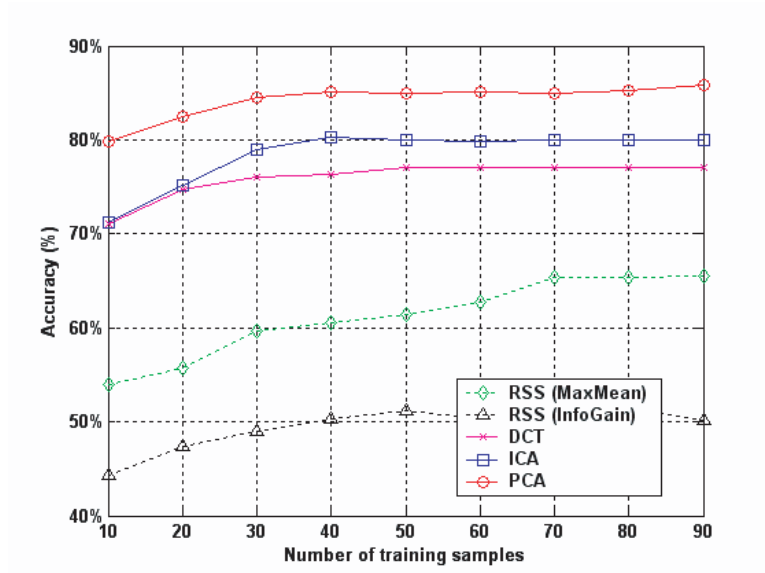
Figure 3.5: Accuracy within 3.0 meters versus number of training samples

computation saving condition. As can be seen, at an error distance of 3.0 meters, the accuracy increased from 65.46% to 85.81% in PCA space. At the same time, the online computation complexity is still reduced and leads power efficient in the client side.

From an implementation perspective, the calculation of the exponential function $e(\cdot)$ can be computed with a pre-stored table in the memory to speed the positioning. In such a case, the power consumption of the positioning software can be further reduced.

3.3.4 Reduction in Human Effort

The limitation of all location fingerprinting systems is that it requires site survey to collect RSS data in order to build the radio map in the initialization and training phase. Data collection can account for large part of the cost of developing a location fingerprinting system. In this experiment, we use only the random

subset of the training samples at each location. The number of training samples at each location varies from 10 to 90, and we plot the accuracy at error distance 3.0m under 3 APs case. The results in Fig. 3.5 clearly show that the size of training samples can be greatly reduced in the decorrelated space. By using only 10 samples at each location, decorrelated space can even outperform RSS space that use full training samples. Therefore the cost of collecting data is accordingly reduced since the time required for site survey is decreased. The reason is the same as mentioned in the previous sections. That is, the PCA-based location technique utilizes information more efficiently in the projected space. In this way, the extracted features have provided sufficient information for the model learning, and thus less training samples are required in the location system. Again, PCA achieves the best performance, where the accuracy is 84.53% while the DCT and ICA are 76.05% and 78.95% when 30 training samples are utilized. It is also because of the rule provided by PCA, where the basis is ranked from an information-theoretical viewpoint.

3.4 Analysis

In this section, an analytical analysis is provided to observe the effect of the transformation. Fig. 3.6 shows a typical example, where the x-axis and y-axis represent the measurements from two APs, denoted as x_1 and x_2. Each node means the collected RSS at different locations, denoted as L_i. When a new observation comes, the distance between each node is calculated. As can be seen, the nearest location to the observation is L_4 in original RSS space whereas that is L_2 while projecting to ϕ_1. This is our main motivation to purpose the
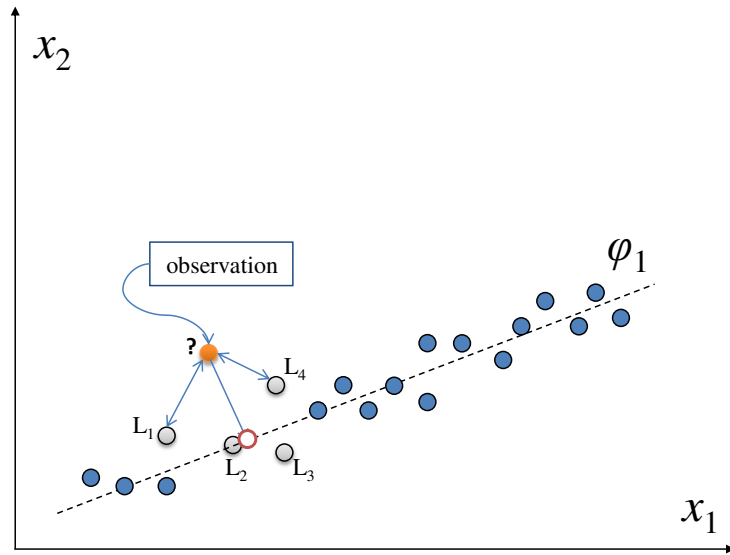
Figure 3.6: An analytic example for the transformation approach.
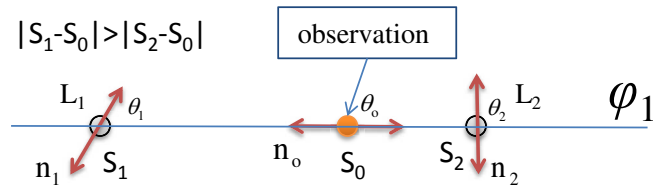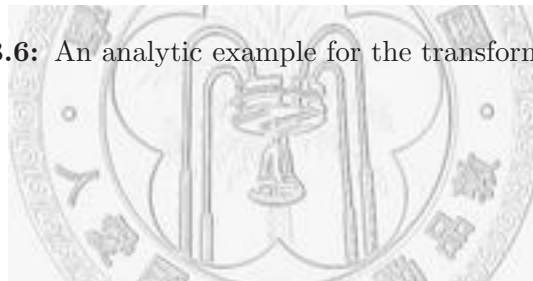
n_1, n_2, n_o are independent and identically-distributed

Gaussian random variables $N(0, \sigma^2)$

Figure 3.7: Analytic geometry for the error probability from the view point of ϕ_1. The error occurs when the observation is decided to belong to L_1.

transformation technique because the direction of ϕ_1 can more clearly reflect the changing distance. Afterwards, we provide an analytic geometry for the error probability from the view point of the signal to noise ratio.

Now, we consider the scenario of the transformed ϕ_1, as shown in Fig. 3.7. We assume that the measurements from L_1 and L_2 are S_1 and S_2, respectively. The observation O is assumed S_0 from the location near L_2 because we set $|S_1 - S_0| \geq |S_2 - S_0|$. Then, the problem can be formulated as a binary classification question: whether the measurement O belongs to L_1 or L_2. In a noise-free case, it is easy to decide since the geometric distance is perfectly estimated. The geometric distance between the measurement O to S_1 and S_2 are denoted as D_{O1} and D_{2O}, respectively. In this case, we definitely choose L_2 for 100% percentage because $D_{O1} = |S_0 - S_1|$ is always larger than $D_{2O} = |S_2 - S_0|$. However, there exists an error probability if we consider the noise. Now, the noise n_1, n_2 and n_o representing the uncertainty are added to the measurements of L_1, L_2 and O individually with the angles θ_1, θ_2 and θ_o. Then the error will occur when $D_{2O} > D_{1O}$. Considering the case in Fig. 3.7, the three measurements can be represented by $(S_1 + n_1 cos(\theta_1), n_1 sin(\theta_1))$, $(S_0 + n_o cos(\theta_o), n_o sin(\theta_o))$ and $(S_2 + n_2 cos(\theta_2), n_2 sin(\theta_2))$.

Defining the four variables $\alpha = n_o cos(\theta_o) - n_1 cos(\theta_1)$, $\beta = n_o sin(\theta_o) - n_1 sin(\theta_1)$, $\gamma = n_2 cos(\theta_2) - n_o cos(\theta_o)$ and $\delta = n_2 sin(\theta_2) - n_o sin(\theta_o)$, the geometric distance D_{1O} and D_{2O} can be represented by $\sqrt{(S_0 - S_1 + \alpha)^2 + \beta^2}$ and $\sqrt{(S_2 - S_0 + \gamma)^2 + \delta^2}$, respectively. Thus, one may derive the following error probability as

$$
\begin{aligned}
P(e) &= P(D_{2O} > D_{1O}) \\
&= P(D_{2O}^2 > D_{1O}^2) \\
&= P((S_2 - S_0 + \alpha)^2 + \beta^2 > (S_0 - S_1 + \gamma)^2 + \delta^2) \\
&= \int_{(S_2 - S_0 + \alpha)^2 + \beta^2 > (S_0 - S_1 + \gamma)^2 + \delta^2} f(\alpha, \beta, \gamma, \delta) d\alpha d\beta d\gamma d\delta \qquad (3.11)
\end{aligned}
$$

However, computing the integration in Eq.3.11 is difficult. Therefore, we only discuss some special cases in the following numerical results.

First, we assume that the noises are independent and identically-distributed (i.i.d.) Gaussian random variables $N(0, \sigma^2)$ and the angles are an identical constant θ, where σ^2 represents the variance. This way, Eq.3.11 is reduced to

$$
P(e) = \int_{(S_2 - S_0 + x\cos(\theta))^2 + (x\sin(\theta))^2 > (S_0 - S_1 + y\cos(\theta))^2 + (y\sin(\theta))^2} f(x, y) dx dy \qquad (3.12)
$$

where $x = n_2 - n_o$ and $y = n_o - n_1$ are both $N(0, \sqrt{2}\sigma^2)$ with the correlation coefficient $\rho_{xy} = 0.5$. Thus, the pdf in Eq.3.12 can be written as

$$
f(x, y) = \frac{1}{\sqrt{3}\pi\sigma^2} \exp(\frac{-2}{3\sigma^2}[x^2 - xy + y^2]) \qquad (3.13)
$$

Note that the joint pdf $f(x, y)$ is a symmetrical sphere where the radius is determined by the variance σ^2, as shown in Fig. 3.8. The impact of θ is showned in Fig. 3.9 where the values of $|S_0 - S_1|$, $|S_2 - S_0|$ and σ are fixed. This figure clearly shows that $P(e)$ is reduced to the minimum value when θ is close to $\pi/2$. That means that the impact of the noise is minimized when the noise angle is vertical to ϕ_1. If we can perfectly separate the signal and noise into two orthogonal directions, then the error probability on ϕ_1 is minimized.
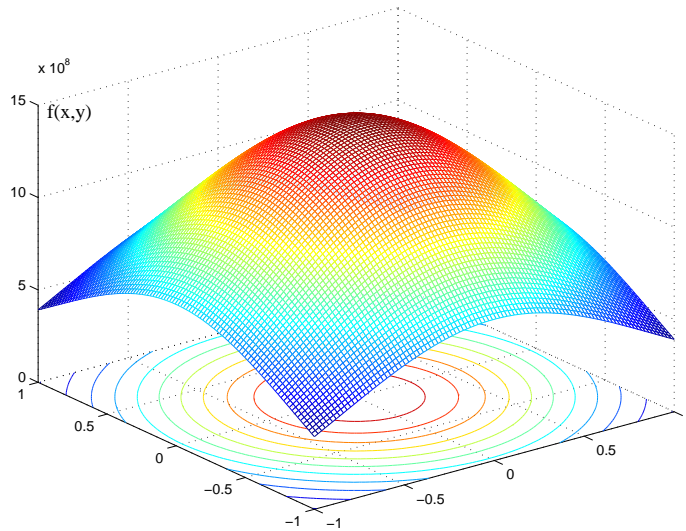
Figure 3.8: The joint probability density function (pdf) of $f(x, y)$ in Eq.3.13. This figure is plotted under $\sigma^2 = 1$.
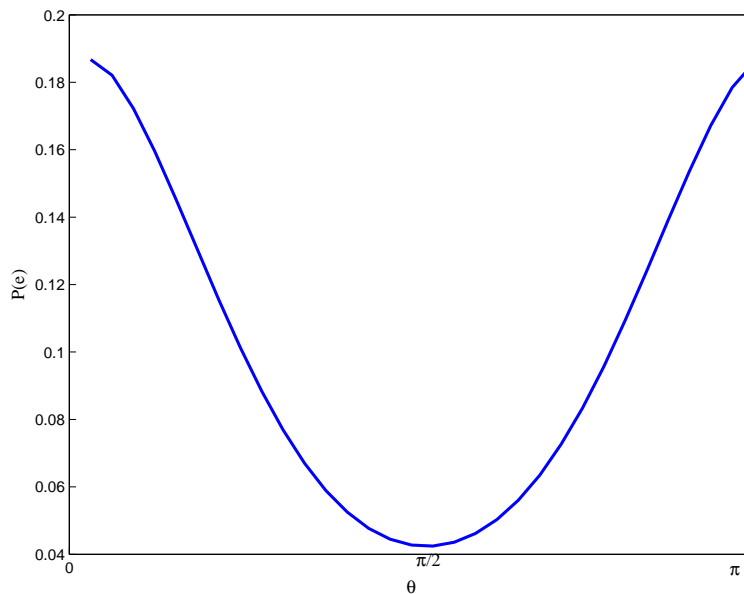
Figure 3.9: The impact of the noise angle θ on $P(e)$. This figure is plotted under $|S_0 - S_1| = 2$, $|S_2 - S_0| = 1$ and $\sigma = 1$.

Consequently, we discuss the error probability under this optimized case ($\theta = \pi/2$) in a further step. When $\theta = \pi/2$, Eq.3.12 is reduced to

$$P(e) = \int_{x^2+y^2>\Delta S_{01}^2-\Delta S_{20}^2} f(x,y)dxdy \qquad (3.14)$$

where $\Delta S_{01} = |S_0 - S_1|$ and $\Delta S_{20} = |S_2 - S_0|$. In this case, the integral range is inside the hyperbolic functions, as shown in Fig. 3.10. From Fig. 3.10, the radius of the circle is directly proportional to σ^2 and the focus of the hyperbola is proportional to $\Delta S_{01}^2 - \Delta S_{20}^2$. Hence, it is clear that $P(e)$ increases as σ^2 increases and decreases with increasing $\Delta S_{01}^2 - \Delta S_{20}^2$. In Fig. 3.11, $P(e)$ versus $\Delta S_{01}^2 - \Delta S_{20}^2$ is drawn for several different values of σ^2 while that is depicted for different θ in Fig. 3.12. Both Fig. 3.11 and Fig. 3.12 confirm the dependences of $P(e)$ vs. $\Delta S_{01}^2 - \Delta S_{20}^2$ and σ^2. From the above analysis, one may deduce that $P(e)$ decreases with increasing $\frac{\Delta S_{01}^2-\Delta S_{20}^2}{\sigma^2}$. Thus, this value can be viewed as a different form of signal-to-noise ratio (SNR). The denominator is in fact the variance of the noise while the numerator indicates the difference of the measured signal between L_1 and L_2. The larger difference indicates the more signal because the greater variability is observed to tolerate the noise. That is why the above metric can be used to characterize SNR in the location task.

It is important to note that this analysis has examined only one direction and noise under two locations condition. Considering a multivariate multiple regression case, one of the most appropriate parameter that can reflect the term $\Delta S_{01}^2 - \Delta S_{20}^2$ is the *variance* in probability theory and statistics. The variance is one measure of statistical dispersion, which captures the RSS's scale or degree of being spread out among different locations in average. This way, the SNR variance ratio can imply the term $\frac{\Delta S_{01}^2-\Delta S_{20}^2}{\sigma^2}$ in some sense. Fortunately, the
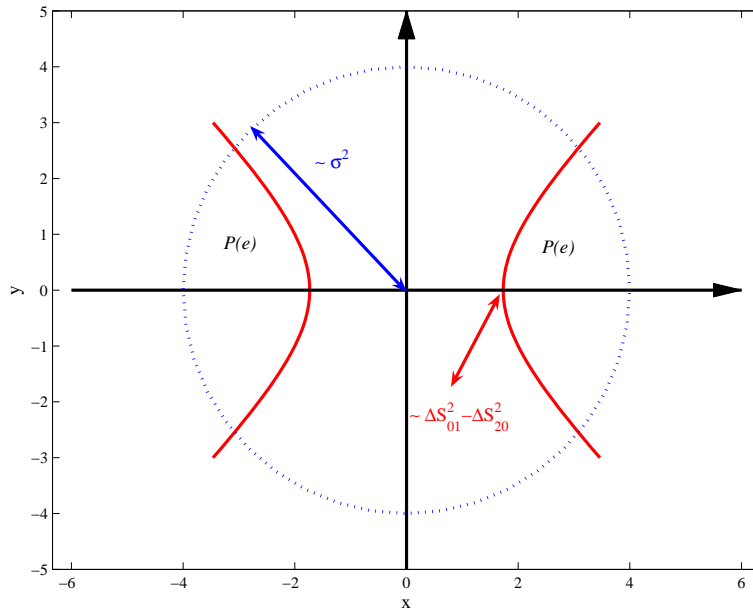
Figure 3.10: A visual picture of the solution in Eq.3.14, where the integral area is inside the hyperbolic functions. This figure is plotted under $\theta = \pi/2$, $\Delta S_{01}^2 = 2$, $\Delta S_{20}^2 = 1$ and $\sigma = 1$.
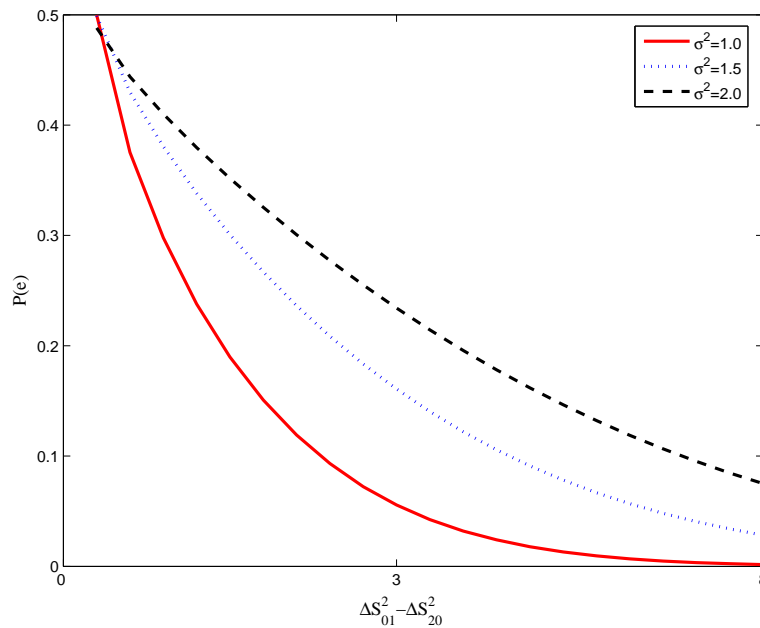
Figure 3.11: The numerical result of $P(e)$ versus $\Delta S_{01}^2 - \Delta S_{20}^2$ for several different values of σ^2, where $\theta = \pi/2$.
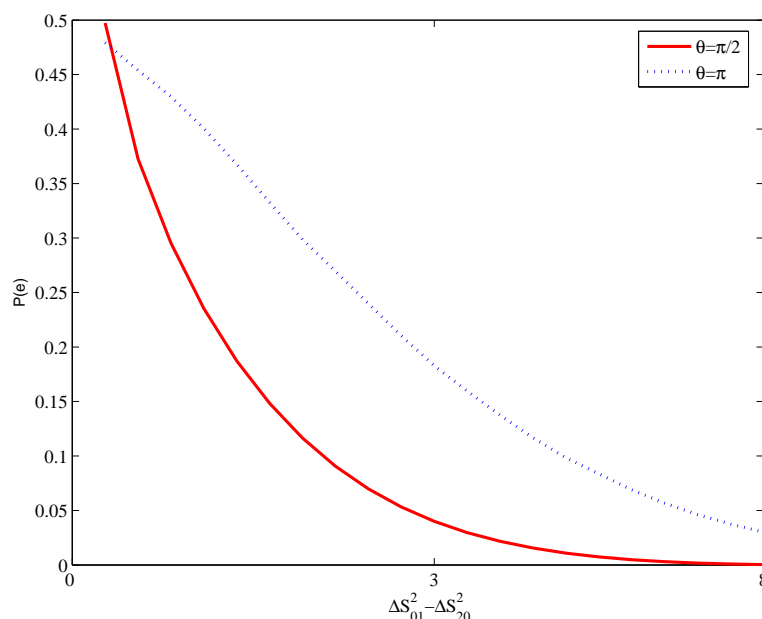
Figure 3.12: The numerical result of $P(e)$ versus $\Delta S_{01}^2 - \Delta S_{20}^2$ for different θ, where $\sigma^2 = 1$.

direction ϕ_1 obtained by PCA can guarantee that ϕ_1 maximizes the SNR variance ratio. In other words, our transformation can be viewed as different filters where the output containing the highest SNR variance ratio is extracted. The advantage of maximizing the SNR variance ratio can be briefly proved as follows.

Let $\mathbf{X} = \mathbf{S} + \mathbf{N}$, where $\mathbf{X}$ is the measured RSS vector, and $\mathbf{S}$ and $\mathbf{N}$ are, respectively, the vector of the clean RSS and additive noise. Assume $\mathbf{S}$ and $\mathbf{N}$ are uncorrelated, the signal-to-noise variance ratio after the transformation is

$$
\begin{aligned}
SNR &= \frac{\text{var}(\phi_1' \mathbf{S})}{\text{var}(\phi_1' \mathbf{N})} \\
&= \frac{\text{var}(\phi_1' \mathbf{X})) - \text{var}(\phi_1' \mathbf{N})}{\text{var}(\phi_1' \mathbf{N})} \\
&= \frac{\text{var}(\phi_1' \mathbf{X}))}{\text{var}(\phi_1' \mathbf{N})} - 1
\end{aligned}
\tag{3.15}
$$

3. FINGERPRINTING IN A TRANSFORMED SPACE

If the noise is assumed to have an uniform effect on each direction, that is, the covariance of the noise vector $\mathbf{N}$ can be assumed as $\sigma^2\mathbf{I}$, where σ^2 is the variance for each component of $\mathbf{N}$ and $\mathbf{I}$ represents the identity matrix. The term in the denominator of Eq.3.15 becomes

$$
\begin{aligned}
var(\phi_1'\mathbf{N}) &= \phi_1' \cdot cov(\mathbf{N}) \cdot \phi_1 \\
&= \sigma^2 \cdot \phi_1' \cdot \phi_1 \\
&= \sigma^2
\end{aligned}
\tag{3.16}
$$

Now we utilize two properties of PCA to analyze the ability of noise reduction. First, the basis in the transformed space is orthonormal, ($\phi_i' \cdot \phi_i = 1$). Thus, the term $var(\phi_1'\mathbf{N})$ in Eq.3.15 is a fixed value, as indicated by Eq.3.16. Second, the principal components optimize the algebraic property in a maximum variance sense [94–96] as

$$
\phi_1 = \underset{||\phi_1||=1}{\arg\max} \left\{ var(\phi_1'\mathbf{X}) \right\}
\tag{3.17}
$$

In such a case, the numerator term $var(\phi_1'\mathbf{X})$ in Eq.3.15 is maximized by PCA and thus the signal-to-noise variance ratio is also maximized accordingly.

Then, we can prove that the maximum value of $var(\phi_1'\mathbf{X})$ is in fact λ_1 and is attained when $\phi_1 = e_1$. Recall that the covariance matrix of $\mathbf{X}$ is $\mathbf{S}_\Sigma$, and the first principal component is $\mathbf{Y}_1 = \phi_1'\mathbf{X}$, as shown in Eq.3.4 and Eq.3.2. Therefore, the variance of the first principal component is given as:

$$
var(\phi_1'\mathbf{X}) = \phi_1'\mathbf{S}_\Sigma\phi_1
\tag{3.18}
$$

46

Since $\mathbf{S}_\Sigma$ is a real-symmetric matrix, the eigenvectors is orthonormal, $e_1' \cdot e_1 = 1$. Accordingly, one may derive the following results for $\mathrm{var}(\phi_1'\mathbf{X})$.

$$
\begin{aligned}
\arg\max_{||\phi_1||=1} \frac{\phi_1'\mathbf{S}_\Sigma\phi_1}{\phi_1'\phi_1} &= \lambda_1 \\
&= e_1'\mathbf{S}_\Sigma e_1 \\
&= \mathrm{var}(\phi_1'\mathbf{X}) \qquad (3.19)
\end{aligned}
$$

Furthermore, the correlation coefficient between the i-th principal component $\mathbf{Y}_i$ and the k-th RSS $\mathbf{X}_k$ can be obtained by

$$
\rho_{\mathbf{Y}_i,\mathbf{X}_k} = \frac{e_{ik}\sqrt{\lambda_i}}{\sqrt{\sigma_{kk}}}, i, k = 1, 2, \cdots, D \qquad (3.20)
$$

where e_{ik} is the k-th component of the i-th eigenvector and σ_{kk} is the variance of the k-th RSS $\mathbf{X}_k$. This value indicates how much percentage of ϕ_i that $\mathbf{X}_k$ contributes. The larger value imples that ϕ_i is more related to $\mathbf{X}_k$. Eq.3.20 is proved as follows. Let $\mathbf{a}_k' = [0 \ldots 010 \ldots 0]$ so that $\mathbf{X}_k = \mathbf{a}_k'\mathbf{X}_k$. Then the covariance of $\mathbf{X}_k$ and $\mathbf{Y}_i$ can be written as:

$$
\begin{aligned}
Cov(\mathbf{X}_k, \mathbf{Y}_i) &= Cov(\mathbf{a}_k'\mathbf{X}_k, \mathbf{Y}_i) \\
&= \mathbf{a}_k'\mathbf{S}_\Sigma e_i \\
&= \lambda_i e_{ik} \qquad (3.21)
\end{aligned}
$$

Now applying $\mathrm{var}(\mathbf{Y}_i) = \lambda_i$ and $\mathrm{var}(\mathbf{X}_k) = \sigma_{kk}$ and using Eq.3.21, one finally obtains $\rho_{\mathbf{Y}_i,\mathbf{X}_k}$.

$$
\rho_{\mathbf{Y}_i,\mathbf{X}_k} = \frac{Cov(\mathbf{X}_k, \mathbf{Y}_i)}{\sqrt{\mathrm{var}(\mathbf{Y}_i)}\sqrt{\mathrm{var}(\mathbf{X}_k)}}
$$

$$= \frac{\lambda_i e_{ik}}{\sqrt{\lambda_i}\sqrt{\sigma_{kk}}}$$

$$= \frac{e_{ik}\sqrt{\lambda_i}}{\sqrt{\sigma_{kk}}}, i, k = 1, 2, \cdots, D \tag{3.22}$$

To summarize, because the PCA based transformation finds the projection with the maximum variance, the ratio of the signal-to-noise variance (which can be viewed as a different form of SNR) can be maximized as well when we consider a noisy environment. This can be attributed to the fact that the variance of signal is maximized after projecting, and the variance of noise does not change due to its directionless property. The maximized SNR variance indicates that the more location information is available because the greater variability is observed to tolerate the noise. For reasons mentioned above, one may state that the proposed technique projects RSS to the direction which contains the higher SNR so as to produce more reliable location estimation.

3.5   Summary

This chapter presents a novel approach to the problem of location fingerprinting in wireless environments. The main contribution of this chapter is five folds:

(a) We show that, by projecting the measured signal into a decorrelated signal space, the positioning accuracy is improved since the cross correlation between each RSS is reduced.

(b) We demonstrate that this novel approach achieves a more efficient information compaction and provides a better scheme to reduce online computation. The drawback of RSS selection techniques is overcome since we reduce the dimensionality by combing features. Each component in the decorrelated space is the

linear combination of all RSSs. Therefore a more efficient mechanism is provided to utilize information of all RSSs while reducing the computational complexity.

(c) Experimental results show that the size of training samples can be greatly reduced in the decorrelated space. That is, fewer human efforts are required for developing the system.

(d) We carry out comparisons between RSS and three classical decorrelated techniques including DCT,PCA, ICA in this work. Two RSS selection criteria proposed in literature, MaxMean and InfoGain are also compared. Testing on a realistic WLAN environment, we find that PCA achieves the best performance on the location fingerprinting task.

(e)We provide an analytical analysis to observe the effect of the PCA based transformation from the view point of signal-to-noise ratio. From the analysis, we show that the ratio of the signal-to-noise variance (which can be viewed as a different form of SNR) can be maximized when we consider a noisy environment. Such a property explains why PCA performs the best from the geometry of the error probability.

Chapter 4

Cooperative Eigen-Radio Positioning in Heterogeneous Wireless Networks

In this chapter, we investigate the localization in heterogeneous wireless networks. We describe the problem encountered from homogeneous to heterogeneous and report the traditional RSS-fusion methods at the begining. Then, we proposed two algorithms via a cooperative approach. The first algorithm, called Direct Multi-Radio Fusion, tries to discover the spatial correlation after the information of measurements is reorganized in order to minimize the redundancy among different wireless radio technologies. After the reorganization, each new component contains different amounts of correlation with respect to the location estimation. The other algorithm, called Cooperative Eigen-Radio Positioning, takes a step further to incorporate the spatial discrimination property to efficiently estimate the location information.

4.1 From Homogeneous to Heterogeneous Wireless Networks

With the progress of wireless radio technology, various wireless specifications form the heterogeneous wireless networks (HWNs) nowadays. Those wireless standards are proposed to satisfy different needs of users. In the future, it is important to integrate the heterogeneous networks to provide complete wireless services. The wireless positioning is definitely one of the possibilities. In this section, we focus on the problem of wireless positioning from homogeneous to heterogeneous wireless networks. We also report some existing approaches which try to combine the estimated results from different techologies.

Today's mobile devices offer multiple wireless technologies such as the cellular networks (GSM/2.5G/3G), WLAN and Bluetooth. More technologies, such as DVB (digital video broadcasting) and WiMax (worldwide interoperability for microwave access, IEEE 802.16) are expected to be equipped with the future mobile devices. This will create the opportunity to utilize HWNs to localize the user [12]. The practical benefit is that users can be served with more accurate and fantastic LBSs. Once the multi-radio from HWNs is available, a cooperative positioning mechanism can combine the strength and compensate the limitations of various wireless technologies. For instance, the number of GSM base stations is likely to be limited in a rural area. At such conditions, the performance of an individual GSM-based system is limited due to the finite information. On the contrary, the performance of combining information from multiple network architecture can be easily improved to meet the user's requirement because the abundant information from HWNs can be utilized.

This thesis focuses on the received signal strength (RSS) from heterogeneous wireless networks instead of the different signal features in a homogeneous network [13–15]. Nowadays mobile devices are capable of sensing quantities of available RSS thanks to the high-density development of wireless infrastructures. In other words, the dimension of $\mathbf{X}$ increases. Extracting the location knowledge from such measurements of $\mathbf{X}$ poses a new kind of challenge for a multi-radio-based localization system. For example, the information with respect to the location prediction is duplicated due to the redundancy of the multi-dimensional measurements and thus, leading to biased estimates. In addition, the heterogeneity of signal levels within $\mathbf{X}$ definitely exists due to various wireless technology standards and physical radio properties. Some RSS measurements may possess more relevance to the location estimation while the others may have less relevance. For example, [26] and [85] reported that the stronger RSSs may produce more reliable prediction due to the less noise they contain whereas [27] argued that the discriminating RSSs are more useful. In HWNs, such different orders of power strength further increases the difficulties of estimating accurate $p(\mathbf{l_r}|\mathbf{X})$. For those reasons, a cooperative positioning method should be established in an intelligent manner to achieve a higher accuracy.

Traditional RSS-fusion algorithms try to combine the estimated results from multiple technologies by an average [17] or a minimum mean square error (MMSE) sense weighting, namely SELFLOC (selectively fuses location information) algorithm in [18]. This approach can be formulated as:

$$\hat{l} = w_1 l_1 + w_2 l_2 + w_3 l_3 \qquad (4.1)$$

where $\hat{l}$ is the desired output, l_i is the estimated result from the i-th technology

and w_i is the weights determined in minimizing the mean square error from collected data. The performance can be improved under the assumption that the random error can cancel each other out. However, such combined methods only consider the performance of each network independently. For example, if GSM and DVB are available and GSM performs much better than DVB. Then the weighted result is certainly dominated by GSM. This way, the hidden location information of DVB that can compensate GSM is not exploited effectively due to the much lower weights. While many studies have done on the wireless positioning, fusing multiple information from HWNs for localization is still largely missing.
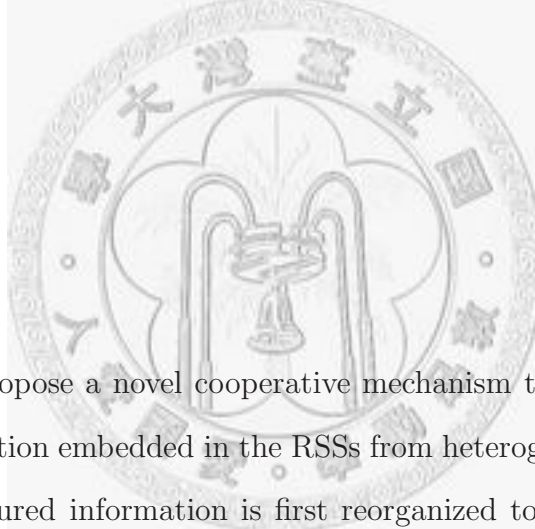
In this chapter, we propose a novel cooperative mechanism to efficiently exploit the location information embedded in the RSSs from heterogeneous wireless radio technologies. Measured information is first reorganized to make sure the repeated information between each other is minimized. Therefore the location information can be more easily exploited. This approach is called Direct Multi-Radio Fusion. Furthermore, each member contains different contents of location information after the reorganization. We take a further step to quantify the location discrimination with respect to each component to efficiently utilize the available information to improve the accuracy performance. This approach is called Cooperative Eigen-Radio Positioning and the two algorithms are described in the following sections.

4.2 Direct Multi-Radio Fusion

Let $\mathbf{T}$ be a decorrelated transformation constructed of the bases as

$$\mathbf{T} = [\phi_1, \phi_2, \cdots, \phi_D]' \tag{4.2}$$

where ϕ_i indicates to the i-th orthonormal basis in $\mathbf{T}$ and the superscript $'$ is the transpose. Such a transformation cancels the duplicated information by combining each RSS in order to more effectively extract the location information.

For convenience, we assume that the device can sense three kinds of RSS including GSM, FM and DVB. The measurements of each network are attached together as

$$\mathbf{X} = [\underbrace{o_1 \cdots o_{d_1}}_{GSM}, \underbrace{o_1 \cdots o_{d_2}}_{FM}, \underbrace{o_1 \cdots o_{d_3}}_{DVB}]' \tag{4.3}$$

where d_1, d_2, and d_3, respectively, represent the number of RSS signals from GSM, FM and DVB and the dimension of the joint vector $\mathbf{X}$ is $D = d_1 + d_2 + d_3$.

Our cooperative location system adopts the kernel-based approach to compute $p(\mathbf{X}|\mathbf{l_r})$ since it reports better result in the recent studies [19]. The probability is assigend to a kernel funciton around each of the observations in the training data, as indicated by Eq. 2.6. Unlike Eq. 2.6, DMRF estimates $p(\mathbf{X}|\mathbf{l_r})$ shown in Eq. 2.4 by incorporating the transformation $\mathbf{T}$. The measurements are reorganized first in the transformed space in order to minimize the duplicate information between different wireless technologies. After substituting Eq. 4.2 into Eq. 2.6, it comes out the transformed-kernel

$$k(\mathbf{TX}, \mathbf{TX_r}(\mathbf{t})) = \exp\left\{\sum_{d=1}^{D} \frac{-1}{2\tilde{\sigma}_{r,d}^2} \left[\phi_d'\mathbf{X} - \phi_d'\mathbf{X}_r(t)\right]^2\right\} \tag{4.4}$$

where $\phi'_d\mathbf{X}$ is the inner product of the d-th basis ϕ_d and the joint observation $\mathbf{X}$ and $\tilde{\sigma}^2_{r,d}$ is the estimated variance of the r-th location and the d-th transformed RSS. Eq. 4.4 illustrates the first contribution of our algorithm where the transformation is integrated into the kernel. This way, the positioning in DMRF is performed by $k(\mathbf{TX}, \mathbf{TX_r(t)})$ instead of $k(\mathbf{X}, \mathbf{X_r(t)})$. Then, DMRF estimates the probabilistic function $p(\mathbf{X}|\mathbf{l_r})$ by non-linearly calculating the transformed kernel distance between $\mathbf{X}$ and all the stored RSS patterns.

$$p(\mathbf{X}|l_r) = \frac{1}{n_r} \sum_{t=1}^{n_r} \hat{K}(\mathbf{TX}, \mathbf{TX}_r(t)) \tag{4.5}$$

After evaluating Eq. 4.5, one may obtain the estimated result by applying it to Eq. 2.4.

If we carefully examine the reorganized information after the projection operation, it will be discovered that the amount of correlation with respect to the spatial prediction for each new member in the projected space $\mathbf{T}$ is different. Some may possess more relevance to the location prediction while the others may have less relevance. In fact, the importance issues among different sources of information have been studied in the literature for the power-efficient WLAN positioning where the more important APs are selected to reduce the computational overhead [26, 27]. In the following, we present another novel algorithm which takes the discrimination property into account such that the likelihood function $p(\mathbf{X}|\mathbf{l_r})$ can be more accurately estimated.
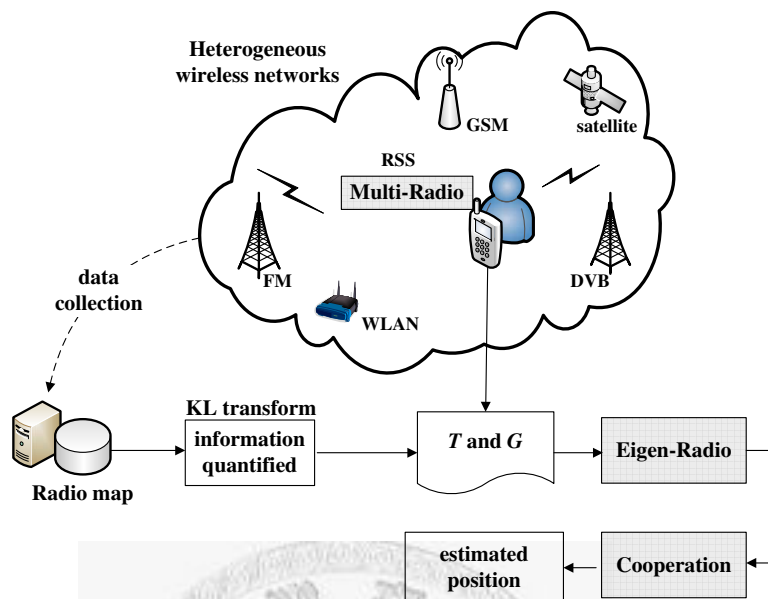
Figure 4.1: The system flow of the proposed cooperative positioning algorithm.

4.3 Cooperative Eigen-Radio Positioning

After the reorganization, the amount of information with respect to the spatial estimation, of each projected direction ϕ_d is quantified in this section. Then, we define the new variables, named *discriminative gains* through a quasi entropy function in order to gracefully incorporate the physical property into the calculation of $p(\mathbf{X}|\mathbf{l_r})$.

Let η_d denote the quantified information for the d-th basis ϕ_d. The more information ϕ_d contains, the more important it is. The importance of ϕ_d should be capable to show the character of distinguishing locations distinctly in the signal space [86]. Therefore, the variance of the projected signals $(\phi'_d\mathbf{X})$ can be a quantified metric to characterize the relevance of location prediction since it explicitly shows the separation of projected RSS over the whole localization area.

Thus, η_d can be defined as follows:

$$\eta_d = \frac{\sum\limits_{r=1}^{R}\sum\limits_{t=1}^{n_r}(\phi_d^{'}\mathbf{X}_r(t) - \bar{\mathbf{X}}_d)^2}{R \cdot n_r} \tag{4.6}$$

where $\bar{\mathbf{X}}_d$, defined as $\frac{1}{R \cdot n_r}\sum\limits_{r=1}^{R}\sum\limits_{t=1}^{n_r}\phi_d^{'}\mathbf{X}_r(t)$, is the global mean of the d-th trans-
formed RSS.

The intuitive reason why the above metric can be used to characterize the
amount of information (importance) in the location estimation can be illustrated
below. A general path loss model can be described as:

$$\overline{PL}(d) \propto (\frac{d}{d_0})^n \tag{4.7}$$

where d_0 is a reference distance, d is the transmitter receiver separation distance
and n is the mean path loss exponent. From Eq. 4.7, the mean path loss $\overline{PL}$ is
a function of distance d to the power of n, which indicates how fast the power
loss increases with the distance. If n is very small and close to 0, RSS is hardly
used to extract the location information because the signal strength does not
change with varying distances. On the other hand, RSS changing at different
locations is evident with a large value of n. That explains why the separation
of projected RSS over the whole localization area can be used to indicate the
amount of information to estimate the location. The larger variance indicates
the more importance because the greater variability of the transformed signal is
observed over the target area.

One practical problem we discover during the experiments is that there ex-
ist large differences of η_d between different projected signals. That is, some η_d
may present several hundred times larger than the other. To provide a graceful

quantitative metric in calculating the spatial likelihood of the measured signals, we utilize a quasi entropy function $f()$ to determine the discriminative gain g_d as follows:

$$
\begin{aligned}
g_d &= \alpha + f(\eta_d) \\
&= \alpha + \frac{-(1 - \eta_d^*) \log(1 - \eta_d^*)}{\beta}
\end{aligned}
\tag{4.8}
$$

where η_d^* is the normalized value of η_d ($\eta_d^* = \eta_d / \sum_{d=1}^{D} \eta_d$) and β is the maximum value of the numerator to make the value of $f(\eta_d)$ smaller than 1 ($\beta = \max(-(1 - \eta_d^*) \log(1 - \eta_d^*))$, $d = 1, 2 \cdots D$). Then, $1 - \eta_d^*$ can be viewed as a numerical value of probability and $f()$ is similar with the definition of entropy function. It can be observed that $f(\eta_d)$ increases with η_d and ranges between 0 and 1 ($0 \leq f(\eta_d) \leq 1$). That means that the changing scale of the discriminate gains is constrained in a reasonable range. In Eq. 4.8, the parameter α is a constant which controls the bias gain. This value is adjusted to make the minimum gain larger than α. This way, the bigger importance η_d is, the larger $f(\eta_d)$ is and the bigger gain g_d is. Moreover, we can control the gains as $\alpha \leq g_d \leq \alpha + 1$ at the same time to avoid an abrupt change on the gains.

Let $\mathbf{G}$ denote the discriminative-gain vector of each ϕ_d. While computing the kernelized distance for the projected signal vector, important ϕ_d are assigned with larger discriminative gains while the less important ones are assigned smaller gains.

$$
\mathbf{G} = \{g_1, g_2, \cdots, g_D\}
\tag{4.9}
$$

In other words, the more important ϕ_d dominates the computation in CERP since they contain strong spatial correlation to produce a more accurate location

4. COOPERATIVE EIGEN-RADIO POSITIONING IN HETEROGENEOUS WIRELESS NETWORKS

estimation. This is the way we devise the cooperation mechanism where each technology is cooperated with its information contribution to estimate the user location.

The location estimation of CERP can be formulated as:

$$\hat{\mathbf{l}} = \sum_{r=1}^{R} \mathbf{l}_r \left(\frac{1}{n_r} \sum_{t=1}^{n_r} \hat{K}(\tilde{\mathbf{T}}\mathbf{X}, \tilde{\mathbf{T}}\mathbf{X}_r(t)) \right) \tag{4.10}$$

where $\hat{K}$ is the projected kernel function shown in Eq. 4.5 and $\tilde{\mathbf{T}}$ represents the joint effect of the discriminative gains $\mathbf{G}$ and the projected operation $\mathbf{T}$. By substituting Eq. 4.8 and $\tilde{\mathbf{T}}$ in Eq. 4.4, the normalized kernel $\hat{K}$ can be obtained

$$\hat{K}(\tilde{\mathbf{T}}\mathbf{X}, \tilde{\mathbf{T}}\mathbf{X}_r(t)) = \exp\{\sum_{d=1}^{D} \frac{-g_d^2}{2\tilde{\sigma}_{r,d}^2} \cdot [\phi_d'\mathbf{X} - \phi_d'\mathbf{X}_r(t)]^2\} \tag{4.11}$$

Eq. 4.10 and Eq. 4.11 illustrate the characteristics of the proposed algorithm. As can be seen, the contribution from each distance member $(\phi_d'\mathbf{X} - \phi_d'\mathbf{X}_r(t))$ is fused with different discriminative gains g_d to estimate the user location. The higher the discriminative gain is, the bigger belief we give to this component which dominates the computation. To our knowledge, such physical property has not been exploited in designing a location system. When the gains are all equal ($g_d=1$, $d = 1 \cdots D$), CERP reduces to DMRF. For the case of $\mathbf{T}=\mathbf{I}$ (an identity matrix), DMRF can be regarded the traditional kernel positioning.

In the following experiments, discrete Karhunen-Loeve (KL) transform is used to determine not only the basis ϕ_d but also the importance η_d from an information theoretical perspective. The KL transform has excellent information packing properties and offers us a tool for quantifying the information [96]. Furthermore, most of the information is squeezed in a relatively lower dimensions to avoid

information redundancies in unnecessary dimensions. That is why KL transform is also known as principal component analysis [23, 95]. The previous chapter has shown that it provides useful decorrelation properties for localization in a homogeneous wireless network [11]. In the KL transformation, each basis ϕ_d can be obtained by finding the eigenvectors $\mathbf{e}_d$ of $\mathbf{S}_\Sigma$ by Eq. 3.4. After getting $\mathbf{e}_d$ from eigen-decomposition of $\mathbf{S}_\Sigma$, RSS can be transformed into the KL space with two advantages. First, the obtained eigenvectors are uncorrelated with each other such that we can avoid measuring the duplicated information. Second, the $\mathbf{e}_i$ is designed to maximize the variance of $\mathbf{e}_d^{'}\mathbf{X}$ subject to $\mathbf{e}_d^{'}\mathbf{e}_d=1$ and the variance of $\mathbf{e}_d^{'}\mathbf{X}$ is in fact the corresponding eigenvalue λ_d. For these reasons, we choose $\phi_d=\mathbf{e}_d$ and $\eta_d=\lambda_d$ in our cooperative positioning algorithms. Because the discriminative gains are determined from the function of eigenvalues, the gained signal is named *eigen-radio* in CERP. As the name indicates, the eigenradio is cooperated each other for accurate localization in HWNs according to its content of location information. The system flow of the proposed CERP architecture is shown in Fig. 4.1.

4.4   Summary

Recent advances in mobile devices and ubiquity of wireless infrastructures create the opportunity to utilize heterogeneous wireless networks for the localization. To efficiently exploit the spatial correlation embedded in the measurements from heterogeneous wireless networks, we proposed two algorithms via a cooperative approach in this chapter. The first is Direct Multi-Radio Fusion (DMRF) where the information is reorganized in a transformed space. The transformation cancels

the duplicated information by combining each RSS such that the location information can be more effectively extracted. The second is Cooperative Eigen-Radio Positioning (CERP) which further takes the spatial discrimination property into consideration. We define the new variables, named discriminative gains through a quasi entropy function in order to gracefully incorporate the physical property into the location estimation. At such a condition, the more important signal with a higher gain dominates the computation in CERP since they contain strong spatial correlation to produce a more accurate location estimation. This is the way we devise the cooperation mechanism where each technology is cooperated with its information contribution to estimate the user location.
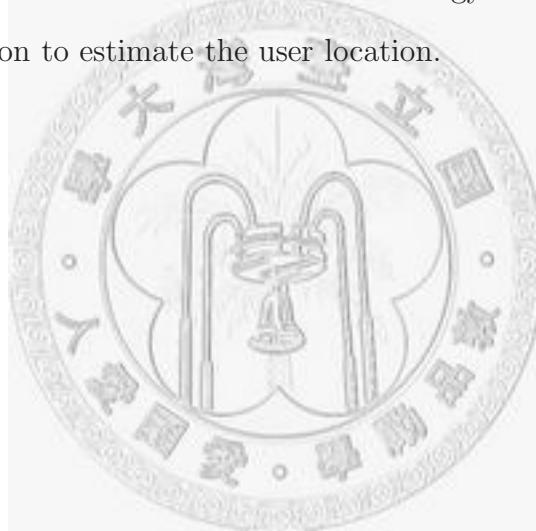
Chapter 5

On-Site Experimental Results

To evaluate the positioning performance of our algorithms, we develop a location fingerprinting system based on heterogeneous wireless networks in this chapter. The sensed radio includes GSM, DVB, FM and WLAN and the experiments are conducted in two different metropolitan-scale environments and one indoor environment including the campus of National Taiwan University (NTU), Wen-Shan rural area and BL building in NTU. In three cases, all the results show that the proposed algorithms outperform the single-network based approaches and SELFLOC in various performance metrics.

5.1 Experimental Setup

We have implemented our algorithms in two metropolitan-scale outdoor environments including the campus of NTU and Wen-Shan District Area, as shown in Fig. 5.1. NTU is located in the south Da-An District of Taipei city, which is the most busiest commercial area in Taiwan. The main campus shown in Fig. 5.1(a) has an area of 1.08 km^2, and is located in the section between an urban and a suburban area with streets, moderate green space and many four to six-story

(a) National Taiwan University (NTU)

(b) Wen-Shan District Area (Wen-Shan)

Figure 5.1: Two different environments where we had performed the experiments include (a) NTU campus and (b) Wen-Shan rural area. The tack indicates the sampling location. Wen-Shan is located near Chi-nan Mountain in the south of Taipei City and its picture is obtained from google-map.
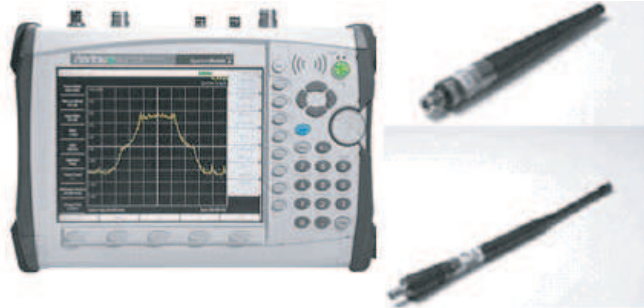
Figure 5.2: Anritsu MS2721B, the commercial available spectrum analyzer we use to record the radio measurements.
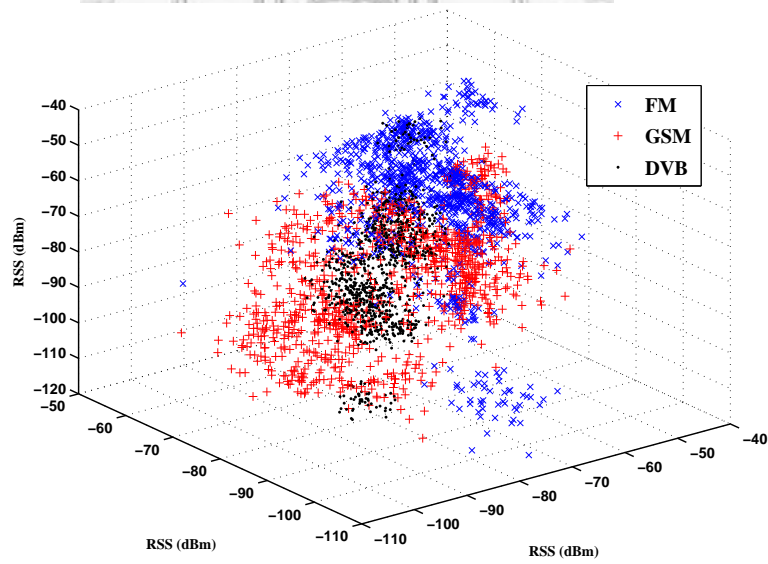

Figure 5.3: A visual picture of the collected GSM, FM and DVB RSS patterns in the NTU campus.

academic buildings. On the other hand, Wen-Shan is a rural area, located near Chi-nan Mountain in the south of Taipei City, as shown in Fig. 5.1(b). There are few high buildings and commercial activities in this area. We measure RSS data at 20 reference locations respectively in these two areas (indicated by the tacks in Fig. 5.1) and collect 100 samples of HWNs for every location. The distance between two neighboring positions ranges from a minimum of 100 m to a maximum of 150 m. We select 50 samples from 15 locations for training data. The testing data is collected 50 samples per location, at 20 locations in different days.

In our experiment, all RSS data are actual measurements obtained by commercially available spectrum analyzer, Anritsu MS2721B, as shown in Fig. 5.2. Three kinds of wireless radio power including GSM, FM and DVB are measured in dBm, as shown in Fig. 5.3. This figure plots the training data of the strongest 3 channels of three technologies. Then, each technology is briefly described as follows. First, GSM is the most popular standard for cellular phones in Taiwan where the networks operate in the 900 MHz or 1800 MHz bands. We focus on 1.8GHz frequency band in this paper because more GSM1800 base stations are provided by network-service providers. We select the 3 strongest RSS for localization from 50 GSM channels range from 1.805 GHz to 1.815 GHz with an interval of 200 kHz (d_1=3). Second, FM is originally designed to listen for broadcasting information such as traffic update. FM uses analog frequency modulation techniques and operates at much lower frequency than GSM. In our test environments, FM containing 36 audible channels distribute from 88 MHz to 108 MHz and the 4 strongest channels are selected (d_2=4). Third, DVB is an open standard for digital television services. In Taipei, the DVB signal contains 10 channels range

from 533 MHz to 599 MHz with an interval of 6 MHz and the 5 strongest channels are used in the experiment (d_3=5). Currently, the DVB service is only provided in an urban area and thus the DVB signal is undetectable in Wen-Shan area.

The GPS system is used as the ground truth and the latitude and longitude are recorded for each reference location. The positioning mode of our device is standard GPS alone and Cartesian coordinate is obtained by WGS84 transformations. The distance between locations is calculated by Great Circle Distance Formula as $r\Delta\sigma$, where r is the great-circle radius of the sphere and $\Delta\sigma$ is the (spherical) angular difference. Based on Vincenty formula, $\Delta\sigma = \arctan(\Phi)$ and Φ is

$$\frac{\sqrt{(\cos\phi_2\sin\Delta\lambda)^2 + (\cos\phi_1\sin\phi_2 - \sin\phi_1\cos\phi_2\cos\Delta\lambda)^2}}{\sin\phi_1\sin\phi_2 + \cos\phi_1\cos\phi_2\cos\Delta\lambda} \tag{5.1}$$

where (ϕ_1, λ_1) and (ϕ_2, λ_2) are the latitude and longitude of two reference locations, $\Delta\lambda$ is the longitude difference and $\Delta\lambda$ is the angular difference.

5.2   Performance Evaluation

Table 5.1: Five error measures (in meters) for different algorithms at NTU campus

Methods	Mean±Standard deviation	Median error	67% CEP	90% CEP
DVB	220.13±111.79	200.34	251.36	387.78
GSM	141.4±114.13	112.93	160.31	328.25
FM	150.89±143.12	108.65	196.41	371.11
SELFLOC	128.56±99.14	98.82	152.49	294.53
DMRF	88.63±100.69	48.30	93.13	282.07
CERP	71.75±102.09	33.82	56.09	259.78

Table 5.2: Five error measures (in meters) for different algorithms at the Wen-Shan rural area

Methods	Mean±Standard deviation	Median error	67% CEP	90% CEP
GSM	169.93±123.43	161.00	221.24	333.32
FM	166.86±144.6	132.14	211.79	408.21
SELFLOC	162.67±114.95	129.06	194.81	342.37
DMRF	104.68±118.44	55.63	123.40	289.85
CERP	95.61±117.51	43.84	100.81	288.89
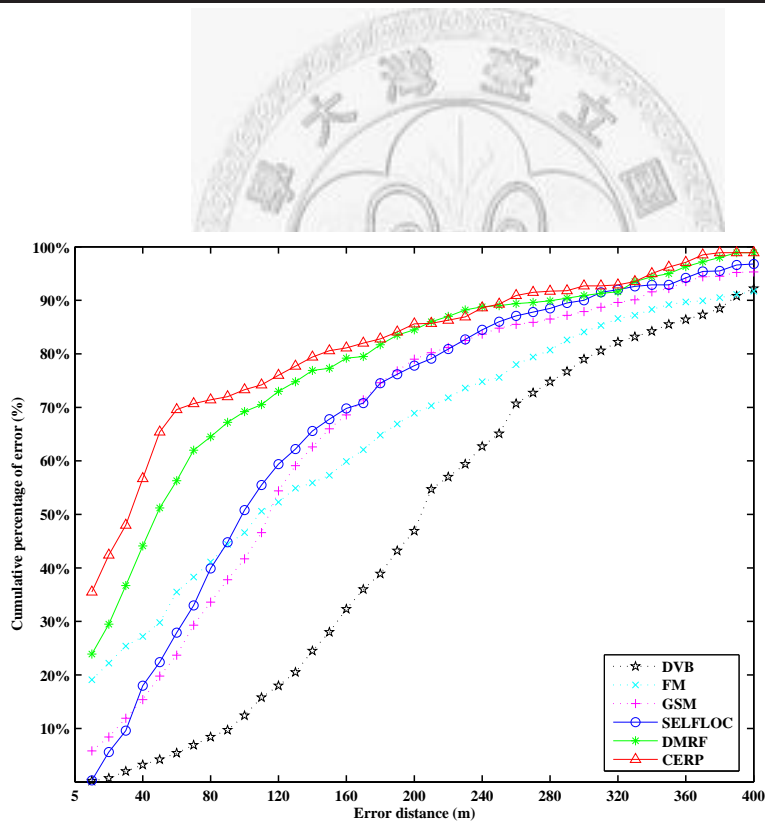
Figure 5.4: Cumulative percentage of error for different algorithms at the NTU campus.

68
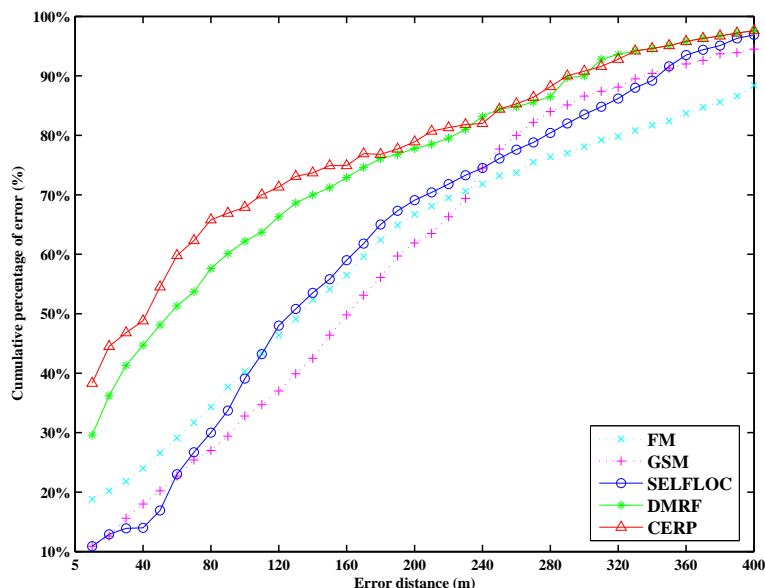
Figure 5.5: Cumulative percentage of error for different algorithms at Wen-Shan rural area.

The performance of our algorithms is evaluated by various error measures in this section. First, the positioning error is defined as the Euclidean distance between the estimated result and the true coordinate as $\varepsilon_i = ||\hat{l}_i - l_i||$, where $\hat{l}_i$ and l_i indicate the i-th estimate and its true location. Then, 6 error measures are reported including standard deviation of error (standard error), mean error, median error, 67% CEP (circular error probable) and 90% CEP. The first 3 measures are defined as standard error $\sigma_\varepsilon = E[(\varepsilon - \bar{\varepsilon})^2]$, mean error $\bar{\varepsilon} = E[(\hat{l} - l)]$ and median error $\tilde{\varepsilon} = \text{median}[(\hat{l} - l)]$. The CEP is defined as the radius of the circle that has its center at the true location and contains the location estimates with probability P_{in} [97]. The last two measures report $P_{in}=0.67$ and $P_{in}=0.90$. Then, each single-network location is estimated by traditional kernel positioning algorithms and SELFLOC is implemented by combing the three estimated results in MMSE sense.
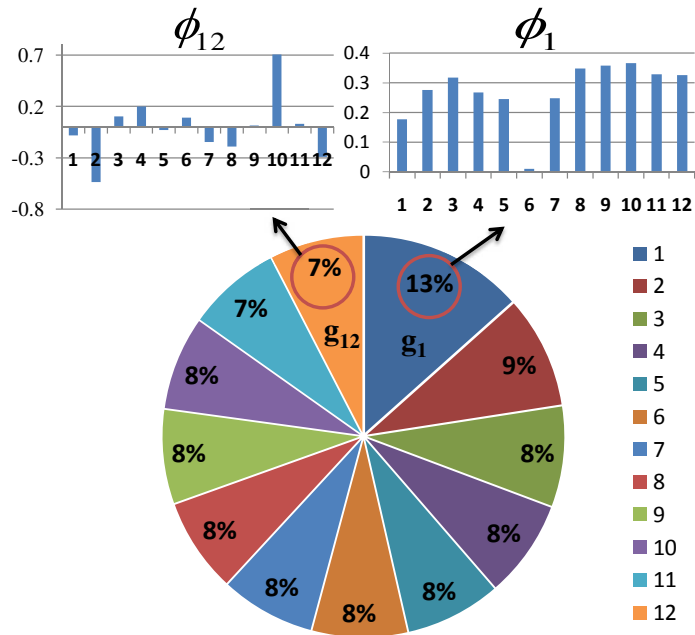
(a) The ratio of the 12 discriminative gains in NTU
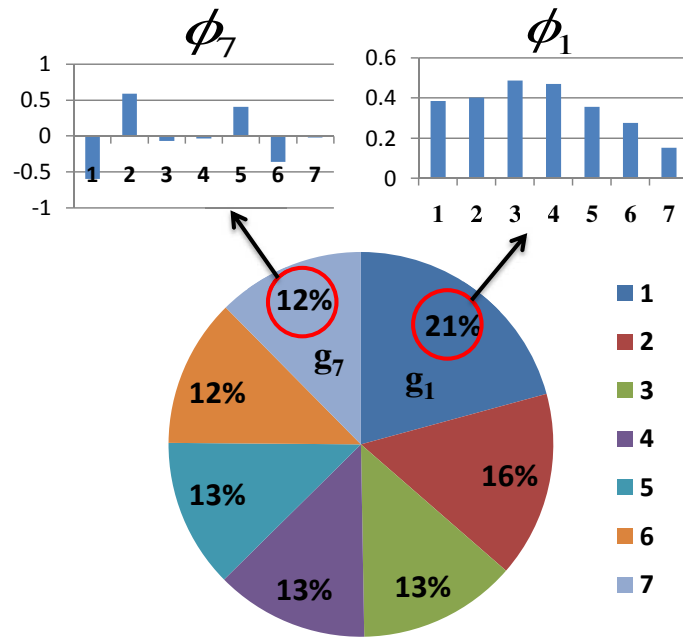
(b) The ratio of the 7 discriminative gains in the Wen-Shan area

Figure 5.6: Analysis of the different discriminative gains in the two experimental areas, where the consant gain α is 1 in both cases.

Table 5.1 reports the five error measures for different algorithms at NTU campus. The table shows that GSM provides the best positioning performance among the three networks. This phenomenon can be explained by Fig. 5.3, where GSM shows the most separative RSS among different locations. The greater discrimination of GSM signal directly reflects on the system performance. The location systems using multiple technologies perform better than the single-network technology. Compared to GSM, SELFLOC exhibits 9.08% and 30.73% reduction in mean and standard error when the estimated results from three networks are combined. Next, we observe that DMRF performs better than SELFLOC. It is because that the information is reorganized to make sure the repeated information between each other is minimized. Therefore the spatial correlation can be more easily exploited in DMRP. More importantly, CERP can further improve DMRF. The significant improvements at mean, median and 67% CEP reduction are 19.05%, 29.98% and 39.77%, respectively. This result can be attributed to that each member after the information reorganization, contains different amounts of location information. CERP take a further step to quantify the location discrimination with respect to each component in order to efficiently utilize the available information to improve the accuracy performance.

To be more specific, Fig. 5.4 graphically depicts the cumulative percentage of error. As can be seen, CERP clearly outperforms DMRF and SELFLOC in terms of the estimated accuracy. Compared with SELFLOC, the discrimibative gains in CERP are embedded on the probabilistic models of each RSS in HWNs instead of the location estimations directly. That is, the contribution of each RSS is different even in a single network while that is uniform in SELFLOC. Compared to DMRF, CERP further takes the spatial discrimination property into consideration. The

discrimibative gains estimated by the quasi entropy function are utilized in CERP such that the location estimation is dominated by the more important eigenradio. Those reasons explain why CERP performs the best theoretically.

The experimental results obtained in Wen-Shan area shown in Table 5.2 and Fig. 5.5. Again, Fig. 5.5 shows that CERP performs the best among the compared algorithms. The results confirm our previous conclusion that the positioning performance can be enhanced if multiple technologies carefully cooperate depending on their discriminative gains. The ratio of the derived discriminative gains in the two experimental areas are plotted in Fig. 5.6. This figure shows that the amount of correlation with respect to the spatial prediction for each new member in the projected space T is different. Some may possess more relevance to the location prediction while the others may have less relevance. The larger gain indicates the more importance because the greater variability of the transformed signal is observed over the target area. It is obvious from Fig. 5.6 that the largest gain g_1 is nearly twice as great as the smallest gain (g_{12} in NTU and g_7 in the Wen-Shan area). It is because that the gains changing is constrained by the quasi entropy function. From Fig. 5.6(a), the first eigen-basis ϕ_1 is combined by almost all RSSs while the same is true of the case in Fig. 5.6(b). On the other hand, the last eigen-basis is usually combined by few RSSs with the lower weights in each case. Those negative values represent the information extraction by canceling the duplication.

Having the above results, one thus now turn to discuss the difference between Wen-Shan and NTU result which lies in the comparison between GSM and FM. From Table 5.1 and Table 5.2, GSM outperforms FM in NTU whereas they present a similar performance in the Wen-Shan area. We discover that the GSM

signal in the rural area is significantly decreasing because of the longer distance to the base stations. Although the signal levels are still much higher than the GSM specification, such signals does not contribute the same location information as that in NTU. On the contrary, FM signal still maintains the same level due to the wider radio coverage. That is why FM produces a comparable performance to GSM in the Wen-Shan rural area.

5.3 Indoor Environments
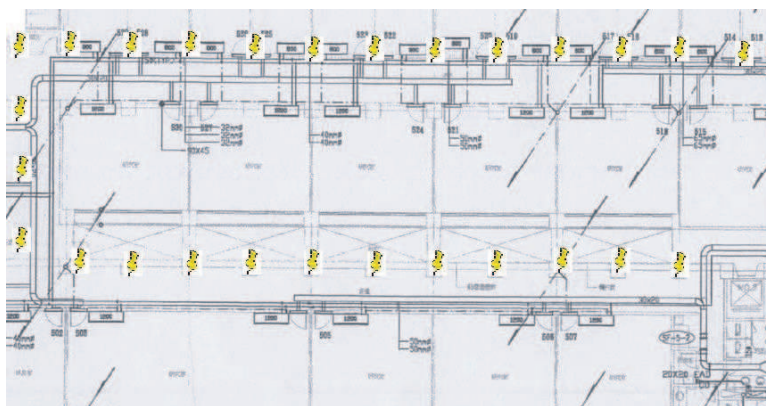
Figure 5.7: Part of the fifth floor plane of the BL building, where we had performed the experiment indoors.

In this subsection, the proposed algorithm is evaluated on indoor environments with an alternative wireless technology. The measurements are collected on the fifth floor of BL building in NTU, as shown in Fig. 5.7. The dimensions of this test-bed are 52 m times 18 m and 35 reference locations are selected with a 3 m space. We follow the same procedure of Section 5.2 to collect 50 samples per location at different time periods for training and testing data, respectively. In addition to GSM, we collect WLAN data in this area by a laptop with Windows XP operating system and NetStumbler network software. Currently, the
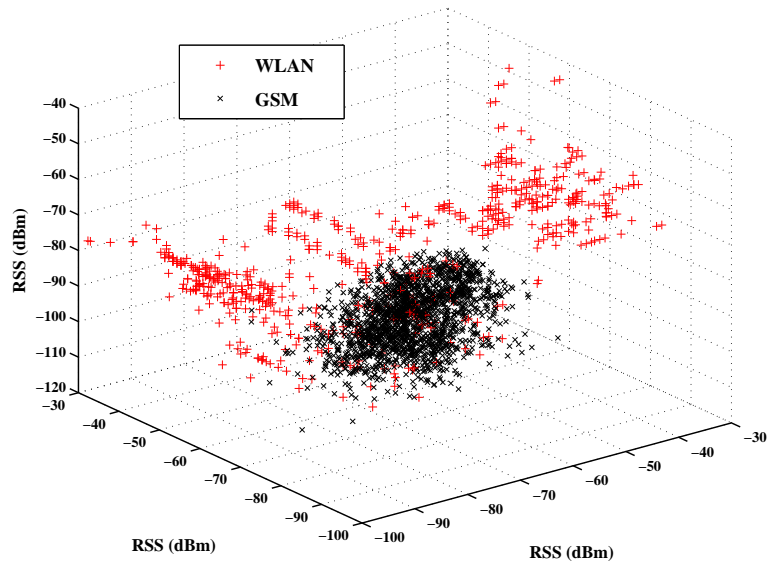
Figure 5.8: A visual picture of the collected WLAN and GSM RSS patterns in the BL building.
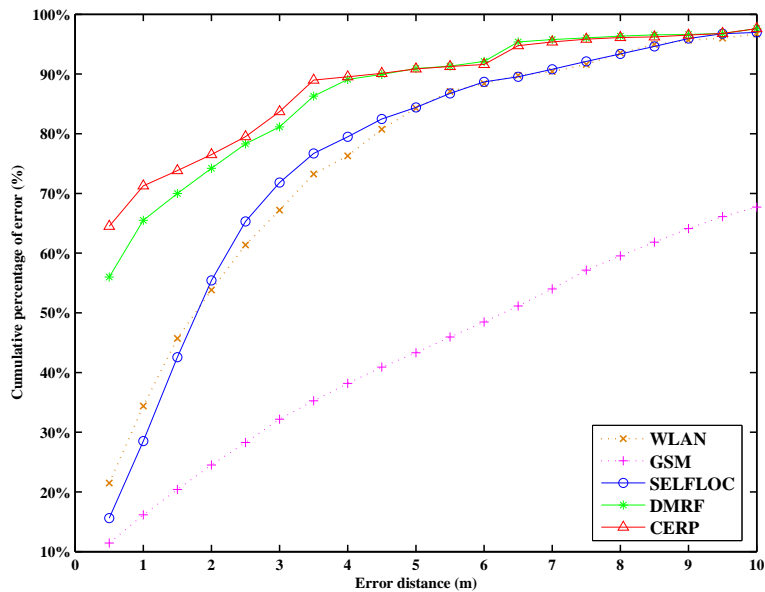
Figure 5.9: Cumulative percentage of error for different algorithms in the BL building.

Table 5.3: Five error measures (in meters) for different algorithms at indoor BL building

Methods	Mean±Standard deviation	Median error	67% CEP	90% CEP
GSM	8.43±8.11	6.32	10.97	20.42
WLAN	2.69±2.99	1.69	2.97	6.56
SELFLOC	2.68±2.83	1.77	2.65	6.65
DMRF	1.48±2.87	0.33	1.19	4.51
CERP	1.37±2.89	0.16	0.87	4.32

infrastructure of WLAN (known as WiFi) is widespread indoors and the function is available in high-level devices such as smart phones and PDA. Our measurements show that over 30 APs can be detected in this floor and the strongest 3 APs are selected to perform the experiment. Fig. 5.8 shows a visual picture of the collected radio in the BL building. This figure clearly presents the asymmetric contribution of GSM and WLAN. As can be seen, WLAN is more important than GSM because WLAN presents better RSS discrimination for the changing distances in this indoor environment. Table 5.3 summaries the experimental results and Fig. 5.9 depicts the accuracy comparisons. As expected, WLAN performs much better than GSM due to its greater variability of RSS over the whole area, as shown in Fig. 5.9. Moreover, the results again verify that our approaches outperform WLAN and SELFLOC. Selecting an appropriate transformation and varying the embedded discriminative gains can achieve the best result, as indicated in Table 5.3. When the gains are estimated by Eq.4.8 in CERP, 51.52% and 26.89% improvements in median error and 67% CEP reduction can be further obtained, as compared to DMRF.

5.4 Summary

In this chapter, we develop a location fingerprinting system based on heterogeneous wireless networks to evaluate the positioning performance of our algorithms. In the first experiment, the sensed radio includes GSM, DVB, FM and the experiments are conducted in two different metropolitan-scale environments including the campus of National Taiwan University (NTU) and Wen-Shan rural area. Both results show that the positioning performance can be enhanced if multiple technologies carefully cooperate depending on their discriminative gains. This is because that the location estimation is dominated by the more important eigenradio, which contains the higher spatial correlation. The significant improvements at mean, median and 67% CEP reduction are 19.05%, 29.98% and 39.77%, respectively.

Then, the proposed algorithm is evaluated on the indoor environments the fifth floor of BL building in NTU, with an alternative wireless technology, WLAN. The results again verify that our approaches outperform WLAN and SELFLOC. Selecting an appropriate transformation and varying the embedded discriminative gains can achieve the best result. When the gains are carefully adjusted by CERP, 51.52% and 26.89% improvements in median error and 67% CEP reduction can be further obtained.

Chapter 6

Conclusions

The demand for location-based services (LBSs) has been driving the need for the accurate positioning techniques in the past and is expected to remain the same in the future. Although Global Positioning System (GPS) has been in service for many years, it is only available in GPS-enable devices and may encounter problems in urban and indoor environments. Thus, the location estimation based on existing wireless communication infrastructures has advanced rapidly in recent years.

At present, one of the most popular RSS-based wireless localization is a two-stage fingerprinting architecture. Location fingerprinting is a promising wireless positioning technology, having the major advantage of providing a high accuracy in challenging wireless environments. The client's position is inferred online by comparing the measured RSS with the offline-constructed fingerprinting model. This approach can be viewed as an application of pattern recognition and thus several statistical learning algorithms have been applied to this problem, as illustrated in chapter 2.

When the positioning algorithm is performed on the handheld devices, extra

care should be taken due to their constrained resource. Therefore, we introduce the concept of transformation in chapter 3. Instead of information selection, the transformation reorganizes the information so as to maximize the retained information while removing parameters as more as possible under the same accuracy constraint. Our algorithm intelligently transforms RSS into a decorrelated space such that the information of all RSSs is more efficiently utilized. We show that, by projecting the measured signal into a decorrelated signal space, the positioning accuracy is improved since the cross correlation between each RSS is reduced. Moreover, we demonstrate that this novel approach achieves a more efficient information compaction and provides a better scheme to reduce online computation. Such a technique is evaluated in a homogeneous wireless network.

Afterwards, we investigate the localization from homogeneous to heterogeneous wireless networks in chapter 4. Due to the ubiquity of heterogeneous wireless networks and the improvements in the device manufacturing, an integrated positioning architecture is envisioned for future multiple-radio computing environments. In chapter 4, we propose a mechanism to efficiently exploit the location information embedded in RSSs from heterogeneous wireless radio technologies. We proposed two algorithms via a cooperative approach. The first algorithm, called Direct Multi-Radio Fusion, tries to discover the spatial correlation after the information of measurements is reorganized in order to minimize the redundancy among different wireless radio technologies. After the reorganization, each new component contains different amounts of correlation with respect to the location estimation. The other algorithm, called Cooperative Eigen-Radio Positioning, takes a step further to incorporate the spatial discrimination property to efficiently estimate the location information. To sum up, we transform

the multiradio first and then further exploit the discriminative gains to produce a more reliable location estimation.

We have implemented our algorithms and evaluated them in chapter 5 by realistic measurements, which are obtained by commercially available spectrum analyzer and wireless cards. The sensed radio includes GSM, DVB, FM and WLAN and the experiments are conducted in two metropolitan-scale and one indoor environment. In three cases, all the results show that the proposed two algorithms outperform the single-network based approaches and SELFLOC in various performance metrics. The results show that the proposed algorithm reduces 44.19-48.88% and 48.25-67.17% of the mean error and 67% CEP, respectively, as compared to SELFLOC.
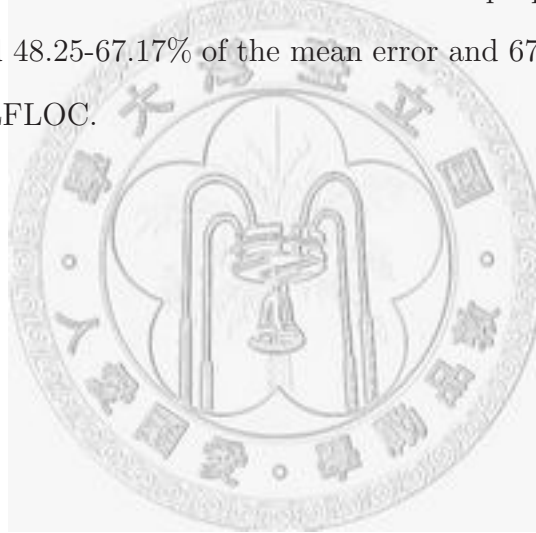
Bibliography

[1] K. Axel, *Location-Based Services : Fundamentals and Operation.* John Wiely & Sons, 2005.

[2] K. W. Kolodziej and J. Hjelm, *Local Positioning Systems: LBS Applications and Services.* CRC Taylor & Francis, 2006.

[3] S. Zafer, G. Sinan, and G. Ismail, *Ultra-wideband Positioning Systems: Theoretical Limits, Ranging Algorithms, and Protocols.* Cambridge, 2008.

[4] F. Gustafsson and F. Gunnarsson, "Mobile positioning using wireless networks: possibilities and fundamental limitations based on available wireless network measurements," *IEEE Signal Processing Magazine*, vol. 22, no. 4, pp. 41–53, 2005.

[5] S. Tekinay, "Wireless geolocation systems and services," *IEEE Communications Magazine*, vol. 36, no. 4, pp. 28–28, 1998.

[6] A. Sayed, A. Tarighat, and N. Khajehnouri, "Network-based wireless location: challenges faced in developing techniques for accurate wireless location information," *IEEE Signal Processing Magazine*, vol. 22, no. 4, pp. 24–40, 2005.

[7] J. Caffery and G. Stuber, "Overview of radiolocation in CDMA cellular systems," *IEEE Communications Magazine*, vol. 36, no. 4, pp. 38–45, 1998.

[8] J. Caffery, J. and G. Stuber, "Subscriber location in CDMA cellular networks," *IEEE Transactions on Vehicular Technology*, vol. 47, no. 2, pp. 406–416, 1998.

BIBLIOGRAPHY

[9] G. Sun, J. Chen, W. Guo, and K. Liu, "Signal processing techniques in network-aided positioning: a survey of state-of-the-art positioning designs," *IEEE Signal Processing Magazine*, vol. 22, no. 4, pp. 12–23, 2005.

[10] K. Pahlavan, X. Li, and J. Makela, "Indoor geolocation science and technology," *IEEE Communications Magazine*, vol. 40, no. 2, pp. 112–118, 2002.

[11] S.-H. Fang, T.-N. Lin, and P.-C. Lin, "Location fingerprinting in a decorrelated space," *IEEE Transactions on Knowledge and Data Engineering*, vol. 20, no. 5, pp. 685–691, 2008.

[12] C.-L. Chen and K.-T. Feng, "Hybrid location estimation and tracking system for mobile devices," *Vehicular Technology Conference*, vol. 4, pp. 2648–2652, 2005.

[13] L. Cong and W. Zhuang, "Hybrid TDOA/AOA mobile user location for wideband CDMA cellular systems," *IEEE Transactions on Wireless Communications*, vol. 1, no. 3, pp. 439–447, 2002.

[14] T. Kleine-Ostmann and A. Bell, "A data fusion architecture for enhanced position estimation in wireless networks," *IEEE Communications Letters*, vol. 5, no. 8, pp. 343–345, 2001.

[15] A. Catovic and Z. Sahinoglu, "The cramer-rao bounds of hybrid TOA/RSS and TDOA/RSS location estimation schemes," *IEEE Communications Letters*, vol. 8, no. 10, pp. 626–628, 2004.

[16] C. Nerguizian, C. Despins, and S. Affes, "Geolocation in mines with an impulse response fingerprinting technique and neural networks," *IEEE Transactions on Wireless Communication*, vol. 5, no. 3, pp. 603–611, 2006.

[17] J. Kwon, B. Dundar, and P. Varaiya, "Hybrid algorithm for indoor positioning using wireless LAN," *Vehicular Technology Conference*, vol. 7, pp. 4625–4629, 2004.

[18] Y. Gwon, R. Jain, and T. Kawahara, "Robust indoor location estimation of stationary and mobile users," *INFOCOM*, vol. 2, pp. 1032–1043, 2004.

[19] A. Kushki, N. Plataniotis, Konstantinos, and N. Venetsanopoulos, Anastasios, "Kernel-based positioning in wireless local area networks," *IEEE Transactions on Mobile Computing*, vol. 6, no. 6, pp. 689–705, 2007.

[20] H. Jeong, J. Kim, and W. K. Cho, "Low-power multiplierless dct architecture using image data correlation," *IEEE Transactions on Consumer Electronics*, vol. 50, no. 1, pp. 262–267, 2004.

[21] A. V. Oppenheim, R. W. Schafer, and J. R. Buck, *Discrete-Time Signal Processing.* New Jersey: Prentice-Hall, 1999.

[22] K. I. Diamantaras and S. Y. Kung, *Principal Component Neural Networks.* New York: John Wiely & Sons, 1996.

[23] R. Duda, P. Hart, and D. Stork, *Pattern Classification.* John Wiely & Sons, 2000.

[24] A. Hyvarinen, J. Karhunen, and E. Oja, *Independent Component Analysis.* New York: John Wiely & Sons, 2001.

[25] R. Gray, *Entropy and Information theory.* New York: Springer-Verlag, 1990.

[26] M. Youssef, A. Agrawala, and A. U. Shankar, "WLAN location determination via clustering and probability distributions," in *Pervasive Computing and Communications*, 2003, pp. 143–150.

[27] Y. Chen, J. Yin, X. Chai, and Q. Yang, "Power-efficient access-point selection for indoor location estimation," *IEEE Transactions on Knowledge and Data Engineering*, vol. 18, no. 7, pp. 877–888, 2006.

[28] A. Smailagic and D. Kogan, "Location sensing and privacy in a context-aware computing environment," *IEEE Wireless Communications [see also IEEE Personal Communications]*, vol. 9, no. 5, pp. 10–17, 2002.

[29] J. Hightower and G. Borriello, "Location systems for ubiquitous computing," *IEEE Computer Magazine*, vol. 34, no. 8, pp. 57–66, 2001.

[30] Y. Zhao, "Mobile phone location determination and its impact on intelligent transportation systems," *IEEE Transactions on Intelligent Transportation Systems*, vol. 1, no. 1, pp. 55–64, 2000.

[31] T. S. Rappaport, J. H. Reed, and D. Woerner, "Position location using wireless communications on highways of the future," *IEEE Communications Magazine*, vol. 34, no. 10, pp. 33–41, 1996.

[32] IEEE, *Part 15.4: Wireless medium access control (MAC) and physical layer (PHY) specifications for low-rate wireless personal area networks (LRW-PANs)*. IEEE P802.15.4a/D4, 2006.

[33] S. Golden and S. Bateman, "Sensor measurements for wi-fi location with emphasis on time-of-arrival ranging," *IEEE Transactions on Mobile Computing*, vol. 6, no. 10, pp. 1185–1198, 2007.

[34] S. Gezici, "A survey on wireless position estimation," *Wireless Personal Communications*, vol. 44, no. 3, pp. 263–282, 2008.

[35] FCC, E911 Decision: Fact Sheet of FCC Wireless 911 Requirements, 2004.

[36] L. Anthony, C. Yatin, C. Sunny, H. Jeffrey, S. Ian, S. James, S. Timothy, H. James, H. Jeff, P. Fred, T. Jason, P. Pauline, B. Gaetano, and S. Bill, "Place Lab: Device positioning using radio beacons in the wild," *Lecture Notes in Computer Science*, vol. 3468, pp. 116–133, 2005.

[37] M. Chen, T. Sohn, D. Chmelev, D. Haehne, J. Hightower, J. Hughes, A. LaMarca, F. Potter, I. Smith, and A. Varshavsky, "Practical metropolitan-scale positioning for GSM phones," in *Ubicomp*, 2006, pp. 225–242.

[38] D.-B. Lin, R.-T. Juang, H.-P. Lin, and C.-Y. Ke, "Mobile location estimation based on differences of signal attenuations for GSM systems," *IEEE Transactions on Vehicular Technology*, vol. 54, no. 4, pp. 1447–1454, 2005.

[39] H. Laitinen, J. Lahteenmaki, and T. Nordstrom, "Database correlation method for GSM location," *Vehicular Technology Conference*, vol. 4, pp. 2504–2508, 2001.

[40] K. John, C. Gerry, and H. Eric, "RightSPOT: A novel sense of location for a smart personal object," in *Ubicomp*, 2003, pp. 36–43.

[41] A. Giordano, M. Chan, and H. Habal, "A novel location-based service and architecture," in *Personal, Indoor and Mobile Radio Communications*, vol. 2, 1995, pp. 853–857.

[42] A. Youssef, J. Krumm, E. Miller, G. Cermak, and E. Horvitz, "Computing location from ambient FM radio signals [commercial radio station signals]," in *Wireless Communications and Networking Conference*, vol. 2, 2005, pp. 824–829.

[43] M. Rabinowitz and J. Spilker, J.J., "A new positioning system using television synchronization signals," *IEEE Transactions on Broadcasting*, vol. 51, no. 1, pp. 51–61, 2005.

[44] H. Namie, K. Nishikawa, K. Sasano, C. Fan, and A. Yasuda, "Development of network-based RTK-GPS positioning system using FKP via a TV broadcast in Japan," *IEEE Transactions on Broadcasting*, vol. 54, no. 1, pp. 106–111, 2008.

[45] J. Yin, Q. Yang, and L. M. Ni, "Learning adaptive temporal radio maps for signal-strength-based location estimation," *IEEE Transactions on Mobile Computing*, vol. 7, no. 7, pp. 869–883, July 2008.

[46] P. Bahl and V. N. Padmanabhan, "RADAR: An in-building RF-based user location and tracking system," in *INFOCOM*, 2000, pp. 775–784.

[47] Y. Moustafa and A. Ashok, "The Horus WLAN location determination system," *Mobile Systems, Applications And Services*, pp. 205–218, 2005.

[48] S.-P. Kuo and Y.-C. Tseng, "A scrambling method for fingerprint positioning based on temporal diversity and spatial dependency," *IEEE Transactions on Knowledge and Data Engineering*, vol. 20, no. 5, pp. 678–684, 2008.

[49] L. T. Son and P. Orten, "Enhancing accuracy performance of Bluetooth positioning," *Wireless Communications and Networking Conference*, pp. 2726–2731, 2007.

[50] G. Mao, B. Fidan, and B. D. O. Anderson, "Wireless sensor network localization techniques," *Computer Network*, vol. 51, no. 10, pp. 2529–2553, 2007.

[51] N. Patwari, J. Ash, S. Kyperountas, I. Hero, A.O., R. Moses, and N. Correal, "Locating the nodes: cooperative localization in wireless sensor networks," *IEEE Signal Processing Magazine*, vol. 22, no. 4, pp. 54–69, 2005.

[52] M. Hazas and A. Hopper, "Broadband ultrasonic location systems for improved indoor positioning," *IEEE Transactions on Mobile Computing*, vol. 5, no. 5, pp. 36–547, 2006.

[53] S. Gezici, Z. Tian, G. Giannakis, H. Kobayashi, A. Molisch, H. Poor, and Z. Sahinoglu, "Localization via ultra-wideband radios: a look at positioning aspects for future sensor networks," *IEEE Signal Processing Magazine*, vol. 22, no. 4, pp. 70–84, 2005.

[54] M. McGuire, K. Plataniotis, and A. Venetsanopoulos, "Location of mobile terminals using time measurements and survey points," *IEEE Transactions on Vehicular Technology*, vol. 52, no. 4, pp. 999–1011, 2003.

[55] X. Li and K. Pahlavan, "Super-resolution TOA estimation with diversity for indoor geolocation," *IEEE Transactions on Wireless Communications*, vol. 3, no. 1, pp. 224–234, 2004.

[56] K. Mikkel, Baun, "A taxonomy for radio location fingerprinting," *Lecture Notes in Computer Science*, vol. 4718, pp. 139–156, 2007.

[57] W. Kim, J. Lee, and G.-I. Jee, "The interior-point method for an optimal treatment of bias in trilateration location," *IEEE Transactions on Vehicular Technology*, vol. 55, no. 4, pp. 1291–1301, 2006.

[58] R. S. Simon and A.-Z. Alejandro, *Antennas and propagation for wireless communication systems*. John Wiely & Sons, 2007.

[59] S. S. John, *Introduction to RF Propagation*. Wiley-Interscience, 2005.

[60] V. V. Saeed, *Advanced Digital signal processing and noise reduction*. John Wiely & Sons, 2006.

[61] S.-H. Fang and T.-N. Lin, "Robust wireless lan location fingerprinting by svd-based noise reduction," *Communications, Control and Signal Processing*, pp. 295–298, 2008.

[62] W.-J. Chang and J.-H. Tarng, "Effects of bandwidth on observable multipath clustering in outdoor/indoor environments for broadband and ultrawideband wireless systems," *IEEE Transaction on Vehicular Technology*, vol. 56, no. 4, pp. 1913–1923, 2007.

[63] Y. Qi, H. Kobayashi, and H. Suda, "Analysis of wireless geolocation in a non-line-of-sight environment," *IEEE Transactions on Wireless Communications*, vol. 5, no. 3, pp. 672–681, 2006.

[64] L. Cong and W. Zhuang, "Nonline-of-sight error mitigation in mobile location," *IEEE Transactions on Wireless Communications*, vol. 4, no. 2, pp. 560–573, 2005.

[65] Y. Qi, H. Kobayashi, and H. Suda, "On time-of-arrival positioning in a multipath environment," *IEEE Transactions on Vehicular Technology*, vol. 55, no. 5, pp. 1516–1526, 2006.

[66] S.-H. Fang, T.-N. Lin, and K.-C. Lee, "A novel algorithm for multipath fingerprinting in indoor WLAN environments," *IEEE Transactions on Wireless Communications*, vol. 7, no. 9, pp. 3579–3588, 2008.

[67] S.-H. Fang, J.-C. Chen, H.-R. Huang, and T.-N. Lin, "Metropolitan-scale location estimation using fm radio with analysis of measurements," *Wireless Communications and Mobile Computing Conference*, pp. 171–176, 2008.

[68] P. Castro and R. Munz, "Managing context data for smart spaces," *Personal Communications, IEEE [see also IEEE Wireless Communications]*, vol. 7, no. 5, pp. 44–46, 2000.

[69] T. Roos, P. Myllymaki, H. Tirri, P. Misikangas, and J. Sievanen, "A probabilistic approach to WLAN user location estimation," *Wireless Information Networks*, vol. 9, no. 3, pp. 155–164, 2002.

[70] P. Krishnan, A. Krishnakumar, W.-H. Ju, C. Mallows, and S. Gamt, "A system for LEASE: Location estimation assisted by stationery emitters for indoor RF wireless networks," *INFOCOM*, vol. 2, pp. 1001–1011, 2004.

[71] Z. li Wu, C. hung Li, J.-Y. Ng, and K. R. Leung, "Location estimation via support vector regression," *IEEE Transactions on Mobile Computing*, vol. 6, no. 3, pp. 311–321, 2007.

[72] R. Battiti, T. L. Nhat, and A. Villani, "Location-aware computing: a neural network model for determining location in wireless LANs," Technical Report DIT-02-0083, Department of Information and Communication Technology, University of Trento, Italy, Tech. Rep., 2002.

[73] A. M. Edgar, C. Raul, and F. Jesus, "Estimating user location in a WLAN using backpropagation neural networks," *Lecture Notes in Computer Science*, vol. 3315, pp. 737–746, 2004.

[74] M. Brunato and R. Battiti, "Statistical learning theory for location fingerprinting in wireless LANs," *Computer Networks*, vol. 47, no. 6, pp. 825–845, 2005.

[75] S.-H. Fang and T.-N. Lin, "Indoor location system based on discriminant-adaptive neural network in ieee 802.11 environments," *IEEE Transactions on Knowledge and Data Engineering*, vol. 19, no. 11, pp. 1973–1978, 2008.

[76] C. Nerguizian, C. Despins, and S. Affes, "Geolocation in mines with an impulse response fingerprinting technique and neural networks," in *Vehicular Technology Conference*, 2004, pp. 3589–3594.

[77] T. King, S. Kopf, T. Haenselmann, C. Lubberger, and W. Effelsberg, "Compass: A probabilistic indoor positioning system based on 802.11 and digital compasses," in *Wireless Network Testbeds, Experimental evaluation and Characterization*, 2006.

[78] C. Patterson, R. Muntz, and C. Pancake, "Challenges in location-aware computing," *Pervasive Computing, IEEE*, vol. 2, no. 2, pp. 80–89, 2003.

[79] V. Otsason, A. Varshavsky, A. LaMarca, and E. de Lara, "Accurate GSM indoor localization," *Lecture Notes in Computer Science*, vol. 3660, pp. 141–158, 2005.

[80] X. Chai and Q. Yang, "Reducing the calibration effort for probabilistic indoor location estimation," *IEEE Trans. on Mobile Computing*, vol. 6, no. 6, pp. 649–662, 2007.

[81] ——, "Reducing the calibration effort for location estimation using unlabeled samples," *Pervasive Computing and Communications*, pp. 95–104, 2005.

[82] L. F. M. de Moraes and B. A. A. Nunes, "Calibration-free WLAN location system based on dynamic mapping of signal strength," in *Mobility management and wireless access*, 2006, pp. 92–99.

[83] K. Mikkel, Baun, T. Georg, and C. Linnhoff-Popien, "Zone-based rss reporting for location fingerprinting," *Lecture Notes in Computer Science*, vol. 4480, pp. 316–333, 2007.

[84] T. King, T. Haenselmann, and W. Effelsberg, "On-demand fingerprint selection for 802.11-based positioning systems," in *a World of Wireless, Mobile and Multimedia Networks*, 2008.

[85] M. Zhang, S. Zhang, and J. Cao, "Fusing received signal strength from multiple access points for WLAN user location estimation," *Internet Computing in Science and Engineering*, pp. 173–180, 2008.

[86] A. Mahtab Hossain, H. N. Van, Y. Jin, and W.-S. Soh, "Indoor localization using multiple wireless technologies," *Mobile Adhoc and Sensor Systems*, pp. 1–8, 2007.

[87] L. Zhang and X. Wu, "Color demosaicking via directional linear mean square-error estimation," *IEEE Trans. Image Processing*, vol. 14, no. 12, pp. 2167–2178, 2005.

[88] S. H. Fang and T. N. Lin, "Indoor localization by a novel probabilistic approach," in *Signal Processing Advances in Wireless Communications*, 2007, pp. 1–4.

[89] J. Pan, J. Kwok, Q. Yang, and Y. Chen, "Accurate and low-cost location estimation using kernels," in *Artificial Intelligent*, 2005, pp. 1366–1370.

[90] J. J. Pan, J. T. Kwok, Q. Yang, and Y. Chen, "Multidimensional vector regression for accurate and low-cost location estimation in pervasive computing," *IEEE Transactions on Knowledge and Data Engineering*, vol. 18, no. 9, pp. 1181–1193, 2006.

[91] A. Hyvarinen, "Fast and robust fixed-point algorithms for independent component analysis," *IEEE Transactions on Neural Networks*, vol. 10, no. 3, pp. 626–634, 1999.

[92] S. Andrew, *Computer Networks*. Prentice-Hall, 1996.

[93] IEEE, *Draft Supplement to Part 11: Wireless Medium Access Control (MAC) and physical layer (PHY) specifications: Medium Access Control (MAC) Enhancements for Quality of Service (QoS)*. IEEE 802.11e/D5.0, 2003.

[94] I.T.Jollife, *Principal Component Analysis*. New York: Springer-Verlag, 2002.

[95] F. Keinosuke, *Introduction to Statistical Pattern Recognition*. Academic Press, 1990.

[96] S. Theodoridis and K. Koutroumbas, *Pattern Recognition*. Academic Press, 2006.

[97] A. J. Weiss, "On the accuracy of a cellular location system based on RSS measurements," *IEEE Transactions on Vehicular Technology*, vol. 52, no. 6, pp. 1508–1518, 2003.